OPEN ACCESS

African Journal of Environmental Science and Technology

June 2021
ISSN 1996-0786
DOI: 10.5897/AJEST
www.academicjournals.org

ACADEMIC JOURNALS
expand your knowledge

About AJEST

African Journal of Environmental Science and Technology (AJEST) provides rapid publication (monthly) of articles in all areas of the subject such as Biocidal activity of selected plant powders, evaluation of biomass gasifier, green energy, Food technology etc. The Journal welcomes the submission of manuscripts that meet the general criteria of significance and scientific excellence. Papers will be published shortly after acceptance. All articles are peer-reviewed

Indexing

The African Journal of Environmental Science and Technology is indexed in:
CAB Abstracts, CABI's Global Health Database, Chemical Abstracts (CAS Source Index), China National Knowledge Infrastructure (CNKI), Dimensions Database, Google Scholar, Matrix of Information for The Analysis of Journals (MIAR), Microsoft Academic

AJEST has an h5-index of 14 on Google Scholar Metrics

Open Access Policy

Open Access is a publication model that enables the dissemination of research articles to the global community without restriction through the internet. All articles published under open access can be accessed by anyone with internet connection.

The African Journal of Environmental Science and Technology is an Open Access journal. Abstracts and full texts of all articles published in this journal are freely accessible to everyone immediately after publication without any form of restriction.

Article License

Memberships and Standards

Academic Journals strongly supports the Open Access initiative. Abstracts and full texts of all articles published by Academic Journals are freely accessible to everyone immediately after publication.

Crossref is an association of scholarly publishers that developed Digital Object Identification (DOI) system for the unique identification published materials. Academic Journals is a member of Crossref and uses the DOI system. All articles published by Academic Journals are issued DOI.

Similarity Check powered by iThenticate is an initiative started by CrossRef to help its members actively engage in efforts to prevent scholarly and professional plagiarism. Academic Journals is a member of Similarity Check.

CrossRef Cited-by Linking (formerly Forward Linking) is a service that allows you to discover how your publications are being cited and to incorporate that information into your online publication platform. Academic Journals is a member of CrossRef Cited-by.

Academic Journals is a member of the International Digital Publishing Forum (IDPF). The IDPF is the global trade and standards organization dedicated to the development and promotion of electronic publishing and content consumption.

Contact

Editorial Office: ajest@academicjournals.org

Help Desk: helpdesk@academicjournals.org

Website: http://www.academicjournals.org/journal/AJEST

Submit manuscript online http://ms.academicjournals.org

Academic Journals
73023 Victoria Island, Lagos, Nigeria
ICEA Building, 17th Floor,
Kenyatta Avenue, Nairobi, Kenya.

Table of Content

Vol. 15(6), pp. 214-222, June 2021
DOI: 10.5897/AJEST2021.2988
Article Number: 6BE0B4966987
ISSN: 1996-0786

http://www.academicjournals.org/AJEST

ACADEMIC JOURNALS
expand your knowledge

African Journal of Environmental Science and Technology

Full Length Research Paper

Determination of the optimum tilt angle for photovoltaic modules in Senegal

Adama Sarr*, Cheikh M. F. Kebe and Ababacar Ndiaye

Laboratoire Eau, Energie, Environnement et Procédés Industriels (LE3PI), Ecole Supérieure Polytechnique (ESP), Université Cheikh Anta Diop de Dakar, Senegal.

Received 1 February, 2021; Accepted 21 May, 2021

This paper deals with finding the optimum tilt angle of solar panels for solar energy applications. The objective is to maximize the output electrical energy of the photovoltaic (PV) modules. A mathematical model was used to determine the optimum tilt angle of solar collectors in Senegal on a daily and monthly basis, as well as for a specific period. Then, the configuration of the optimum tilt angle was analyzed by studying four specific cases in different typical climatic zones in Senegal. On a horizontal plane, the sun spends more time in the south than in the north. This means that in Senegal, the optimum tilt angle is often set equal to latitude. On the other hand, the optimum latitude angle is only for annual optimization. This study shows that the optimum tilt angle equal to latitude does not produce maximum output. For monthly optimum tilt angle, only the month of November gives tilt optimum angles equal to latitude. It is preferable to change the tilt angle of solar conversion systems monthly instead of fixing them, to gain more energy.

Keys words: Solar energy, solar panels, tilt angle, orientation solar panel, latitude, geometry.

INTRODUCTION

Non-renewable energy sources, such as fossil fuel, have been the major source of energy in many countries, including Senegal. However, because of the problems associated with the use of these non renewable energy sources, there is a need for alternative energy sources that are sustainable and nonpolluting. The optimum orientation of a solar conversion system obeys to a simple rule towards the Equator, which gives: orientation to the south in the northern hemisphere (azimuth angle =0°); and orientation to the north in the southern hemisphere (azimuth angle =180°) (Tiris and Tiris, 1998; Ihaddadene and Charik, 2017). Other researchers (Tripathy et al., 2017; Yadav et al., 2021) used models to determine the optimum tilt angle and then studied the influence of the shadow of urban residential buildings on this angle. The monthly optimum tilt angle was calculated in Malaysia by Liu and Jordan method over three rural areas (Fadaeenejad et al., 2015). Using diffuse radiation methods, (Hailu and Fung, 2019) determined the optimum tilt angle in an area located in Canada. In the same context, (Kamanga et al., 2014) calculated the optimum tilt angles for a district in Malawi. In order to optimise solar isolation on solar collectors, appropriate method to determine solar tilt angles at any given time is essential to increase the efficiencies of the collectors and that of the devices connected to them (Idowu et al.,

*Corresponding author. E-mail: adama15.sarr@ucad.edu.sn. Tel. +221770955919.

2013). The optimum tilt angle of solar collectors such as photovoltaic solar panels is important for conversion of solar radiation into heat or electricity (Mahdi et al., 2011). Zang et al. (2016) determined the optimum tilt angle of photovoltaic systems by considering different regional climates in China. To maximise the amount of energy captured by solar collectors, the sun tracking system is often used as an attractive technology for solar collectors or panels (Lv et al., 2018).

A number of studies have been carried out by various investigators in order to optimize the tilt angle around the world (Lewis, 1987; Saraf and Hamad, 1988; Hussein et al., 2000; Shariah et al., 2002; Skeiker, 2009). Optimization of the tilt angle has been performed for various locations in differents countries. In Turkey, Bakirci (2012) determined a general models for optimum tilt angles of solar panels. It is in this same context that (Kacira et al., 2004) used a mathematical model to determine the optimum tilt angle to make the photovoltaic production optimum. A mathematical modeling of the optimum tilt for solar collectors is presented by (Stanciu et al., 2016) for intercepting maximum solar irradiance in Romania. A study in Jordan (Mahmoud and Nabhan, 1990) compared the PV energy produced with the optimum tilt angle to the energy produced with the fixed tilt angle and showed a 5.6% gain in production with the optimum tilt angle determined. In Austria and Germany, Hartner et al. (2015) evaluated the trade-off between annual energy losses and possible electricity generation cost reductions through adapting PV installation angles for the current electricity system and for potentially higher PV penetration levels in the future. In Greece, Mehleri et al. (2010) carried out a study on the determination of the optimum tilt angle and orientation for solar photovoltaic arrays in order to maximize the incident of solar irradiance exposed on the array, for aspecific period of time. For the Asian countries, studies for the modeling of the optimum angle of inclination have also been made. Khahro et al. (2015) evaluated solar energy resources by establishing diffuse solar radiation models and obtaining optimum tilt angle for a prospective location is southern region of Sindh, Pakistan. In Iran, Moghadam et al. (2011) performed optimization of solar flat collector inclination. In Indonesia, (Handoyo et al., 2013) maximized the incidence angle to obtain the tilt optimum angle. In India, Dixit et al. (2017) proposed a particle swarm optimization estimator in order to find optimum tilt angle on annual basis. To restitute solar radiation over 4 climatic zones in Senegal, Sarr et al. (2020a) used as input parameters the meteorological and geographical parameters and also the position of the sun. Eke (2011) revealed that the average angle of inclination at which a flat surface solar collector will be mounted at fixed position in Zaria, Nigeria is 22.5°. Another approach based on in situ measurements also allows to determine the energy produced with optimum tilt angles (Li and Lam, 2007). A study also showed that the optimum tilt angle varies depending on the type of PV technologies used (Ayaz et al., 2017).

Senegal is located on the extreme western tip of the African continent between latitude 12 and 17° north and longitude 10 and 18° west. Solar energy is abundant in Senegal though locally measured data is not available for most locations. Internationally available satellites databases, however, provide sufficient data for most design purposes. Senegal ceives 5.5 kWh/m2/day and an average annual sunshine duration of around 3,000 h (www.aner.sn).

The research question addressed in this paper is concerned with the optimum tilt angle of solar systems to maximize electricity production. Many studies are limited to calculating the monthly or annual optimum tilt angle for a single specific zone. Our study determines the daily, monthly and yearly optimum tilt angle for Senegal and applies them on different zones chosen according to the climate contrast existing between them.

MATHEMATICAL PROCEDURE FOR CALCULATING THE OPTIMUM TILT ANGLE

In Senegal, there is no research on the determination of the optimum tilt angle. This work applies the Kassaby model to calculate the optimum tilt angle over Senegal, that is, between latitudes 12 and 17° north. This model will then be applied in four zones of Senegal (Figure 1) chosen according to their different regional climates. The percentage of daily and monthly variation of the optimum tilt angle is given for each study case. There are other methods to determine the optimum tilt angle, but we chose the Kassaby method. This method consists of determining the optimum daily $\beta_{opt,d}$ and monthly tilt angle $\beta_{opt,m}$. Our goal is to adjust the optimum tilt angle for our solar applications at least once a month to maximize photovoltaic production. The equations $\beta_{opt,d}$ and $\beta_{opt,m}$ are programmed with R software.

Main angles in solar applications

The optimum tilt angle βopt, the declination angle δ and sunset hour angle h_{ss} can be determined by the following equations (El-Kassaby, 1988):

$$\beta_{opt,d} = \phi - \tan^{-1}\left[\frac{h_{ss}}{\sin h_{ss}}\tan(\delta)\right] \quad (1)$$

$\beta_{opt,d}$ is optimum tilt angle at a particular day and ϕ is the latitude of the location.

$$\delta = -23.25\left[\cos(n+10.5)\frac{360}{365}\right] \quad (2)$$

$$h_{ss} = \cos^{-1}[-\tan(\phi)\tan(\delta)] \quad (3)$$

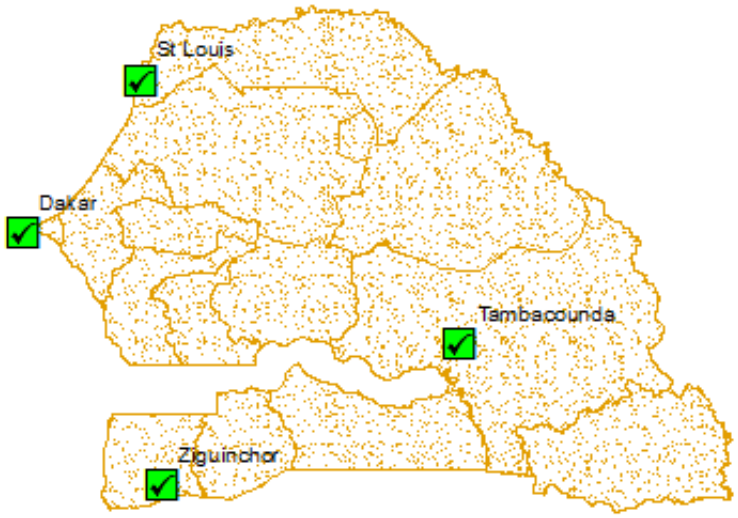

Figure 1. Typical climate zones selected for the study.

The monthly optimum tilt angle is given by :

$$\beta_{opt,m} = \phi - \tan^{-1}\left[\frac{\sum_{n_1}^{n_2}\frac{24}{\pi}I_0\left[1+0.034\cos\left(\frac{2\pi n}{365}\right)\right]\sin(\delta)h_{ss}}{\sum_{n_1}^{n_2}\frac{24}{\pi}I_0\left[1+0.034\cos\left(\frac{2\pi n}{365}\right)\right]\cos(\delta)\sin(h_{ss})}\right] \quad (4)$$

The sunset hour angle for the tilted surface is expressed as:

$$h_{ss} = min\left[\cos^{-1}(-\tan(\phi)\tan(\delta),\ \cos^{-1}(\phi-\beta_{opt,m})\tan(\delta))\right] \quad (5)$$

Where ‘‘min” means the smaller of the two items in the bracket.

RESULTS AND DISCUSSIONS

Daily optimum tilt angle

For photovoltaic solar applications, it is important to know the tilt angle. The latter is calculated according to the temporal variation of the movement of the sun in the sky. The results obtained for different latitude angles are shown in Table 1.

The results show that for a given latitude, the optimum tilt angle ($\beta_{opt,d}$) varies from one day to another. The optimum tilt angle is sometimes greater than latitude and sometimes less than latitude. This phenomenon depends on the day and the month considered. Only the month of February gives optimum tilt angles, which are greater than the latitude for all days.

Application for four typical climatic zones for daily optimum tilt angle

To take into account the climatic zoning, we consider four zones (Figure 1) which are Dakar (14.733° N, 17.467° W) located in the Cape Verde Peninsula, St Louis (16.050° N, 16.450° W) located in the Senegal River Delta, Tambacounda (13.767° N, 13.683° W) located in-land in the south-eastern Senegal and Ziguinchor (12.550° N, 16.267° W) located in the southwest part of Senegal (Sarr et al., 2020b).

Figure 2 shows the results of the variation of the daily optimum tilt angle at Dakar. Except for a few rare days on Dakar where we find optimum tilt angles equal to the latitude, these areas show optimum tilt angles different from the latitude. In Dakar there is a difference of 20.05% between the maximum value of the optimum tilt angle and its minimum value. Latitude has a variance of 11.14% from the minimum value of the optimum tilt angle while this difference is 10.03% from the maximum value of the optimum tilt angle. This difference is significant from the point of view of efficiency. Solar power plants must take into account the optimum tilt angle to optimize their production.

Figure 3 shows the results for St Louis. The difference between the maximum value of the optimum tilt angle and the minimum value of it in St Louis is 18.74%. Between latitude and the minimum value of the optimum tilt angle, the variance is 9.75% while between the maximum value of the optimum tilt angle and latitude the difference is 9.96%.

Figure 4 shows the results for the Tambacounda zone. In Tambacounda, there is a variation of 23.43% between the maximum and minimum values of the optimum tilt angle. Compared to the latitude, the difference is 13.84% from the minimum value of the optimum tilt angle and 11.13% from its maximum value.

The findings for Ziguinchor are shown in Figure 5. The results showed that in Ziguinchor there are a difference of 23.01% between the maximum and minimum values of

Table 1. Daily optimum tilt angle $\beta_{opt,d}$ for different latitude angles of Senegal.

N	Date	Latitude					
		12	13	14	15	16	17
January							
1	1	11.83	12.81	14	15.56	15.81	16.79
15	15	12.19	13.17	14	15.19	16.17	17.1
31	31	11.69	12.67	13.64	14.69	15.67	16.64
February							
32	1	12.19	13.17	14	15.19	16.18	17.1
46	15	13.41	14.41	15.41	16.41	17.41	18.41
59	28	12.87	13.86	15.41	15.87	16.86	17.84
March							
60	1	10.82	11.82	12.8	13.82	14.82	15.81
74	15	12.76	13.75	14.68	15.76	16.75	17.72
90	31	13.11	14.1	15.08	16.11	17.11	18.09
April							
91	1	10.84	11.83	12.81	13.84	14.83	15.82
105	15	13.39	14.39	15.38	16.39	17.34	18.39
120	30	11.68	12.66	13.63	14.69	15.67	16.63
May							
121	1	12.79	13.78	14.7	15.78	16.78	17.74
135	15	10.44	11.44	12.44	13.44	14.44	15.44
151	31	11.72	12.71	13.69	14.73	15.71	16.67
June							
152	1	11.79	12.77	13.81	14.79	17.77	16.74
166	15	10.5	11.5	12.5	13.5	14.5	15.5
181	30	10.57	11.57	12.57	13.57	14.57	15.57
July							
182	1	11.98	12.96	14	14.98	15.96	17
196	15	11.68	12.66	13.63	14.68	15.67	16.63
212	31	11.19	12.18	13.13	14.19	15.18	16.15
August							
213	1	12.24	13.23	14.05	15.25	16.23	17.16
227	15	11.85	12.83	14	14.86	15.84	16.82
243	31	10.44	11.44	12.44	13.44	14.44	15.44
September							
244	1	13.37	14.37	15.36	16.37	17.37	18.36
258	15	12.14	13.12	14	15.14	16.12	17.04
273	30	11.83	12.81	14	14.84	15.82	16.79
October							
274	1	10.48	11.48	12.48	13.48	14.48	15.48
288	15	11.34	12.33	13.28	14.34	15.33	16.3
304	31	10.55	11.55	12.55	13.55	14.55	15.55
November							
305	1	11.41	12.39	13.34	14.41	15.39	16.36
319	15	11	11.2	12.97	14.01	15	15.99
334	30	11.58	12.56	13.51	14.58	15.57	16.53

Table 1. Contd.

December							
335	1	11.11	12.1	13.07	14.11	15.1	16.08
349	15	13.14	14.14	15.12	16.14	17.14	18.13
365	31	13.56	14.56	15.56	16.56	17.56	18.56

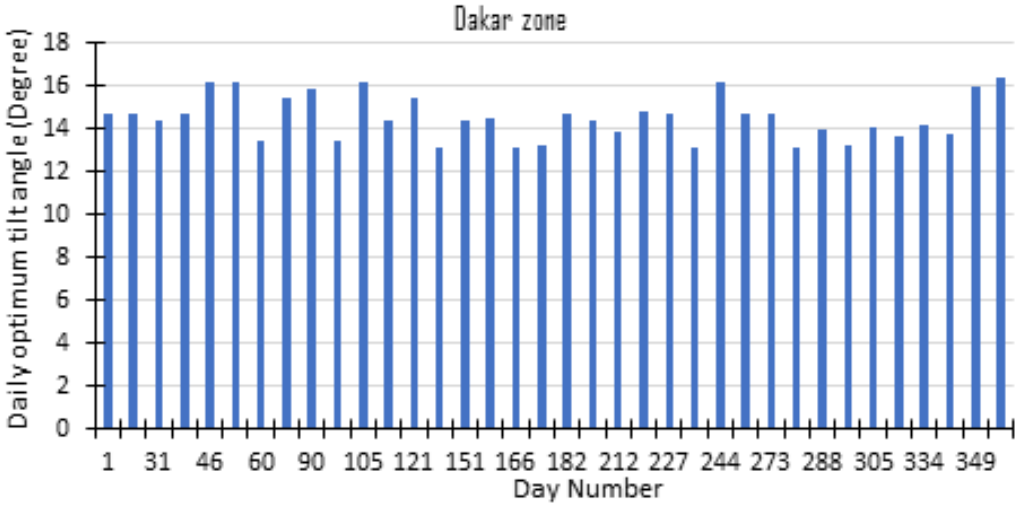

Figure 2. The variation of daily optimum tilt angle, $\beta_{opt,d}$ with the day number n for Dakar.

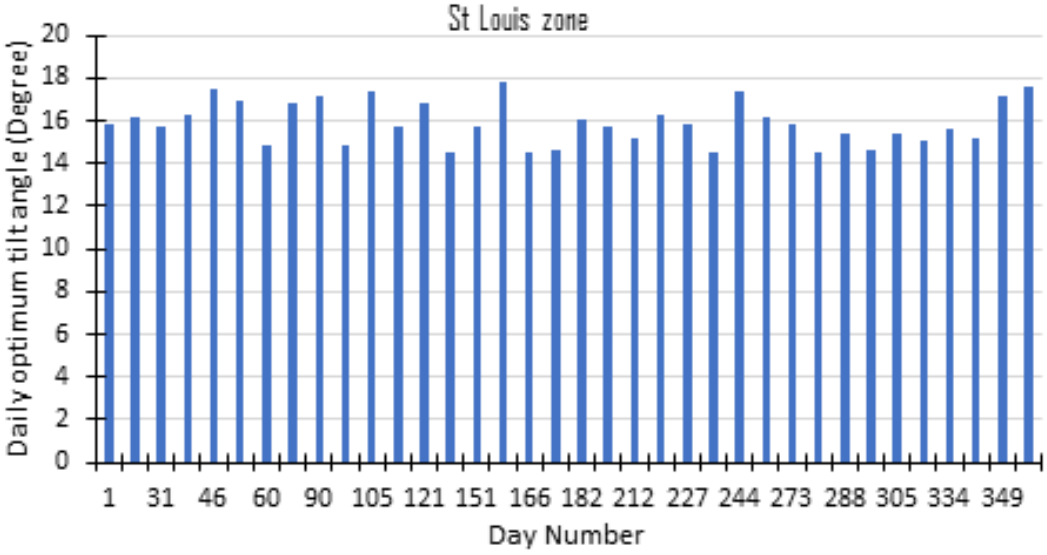

Figure 3. The variation of daily optimum tilt angle, β_(opt,d) with the day number n for St Louis.

the optimum tilt angle. This variance is 13.00% between the latitude and the minimum of the optimum tilt angle while it is 11.50% between the maximum of the optimum tilt angle and the latitude.

Monthly optimum tilt angle

Table 2 represents the monthly optimum tilt angle $\beta_{opt,m}$ for different latitude angles of Senegal. The optimum tilt

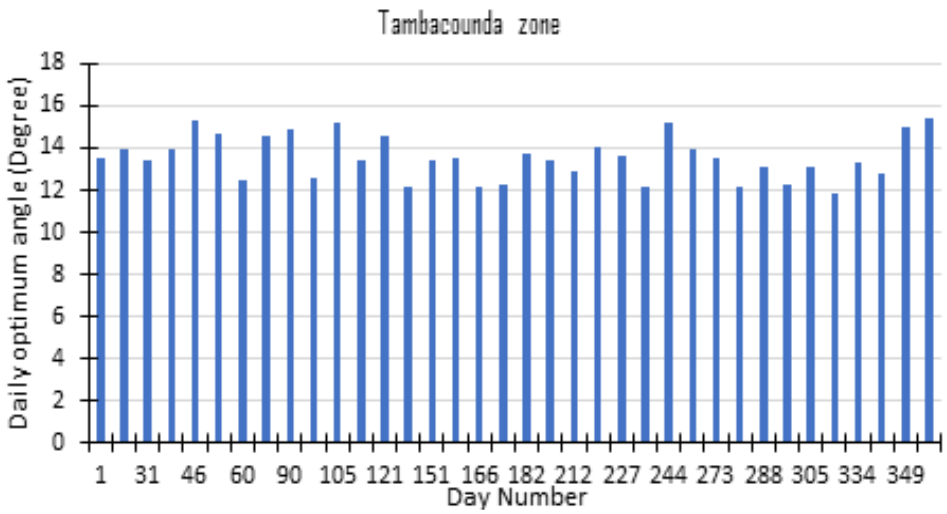

Figure 4. The variation of daily optimum tilt angle, β_(opt,d) with the day number n for Tambacounda.

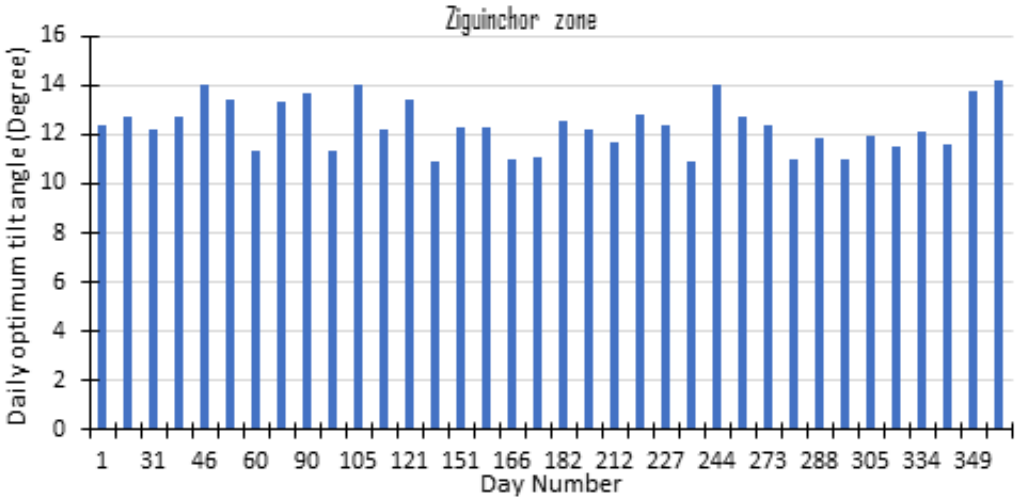

Figure 5. The variation of daily optimum tilt angle, β_(opt,d) with the day number n for Ziguinchor.

Table 2. Monthly optimum tilt angle β_(opt,m) for different latitude angles of Senegal.

Lat.	January	February	March	April	May	June	July	August	September	October	November	December	Year
12	11.63	11.75	11.71	11.62	11.63	11.97	11.89	12.24	12.38	12.36	12	12.18	11.95
13	12.63	12.75	12.71	12.62	12.63	12.97	12.89	13.24	13.38	13.36	13	13.18	12.95
14	13.63	13.75	13.71	13.62	13.63	13.97	13.89	14.24	14.38	14.36	14	14.18	13.95
15	14.63	14.75	14.71	14.62	14.63	14.97	14.89	14.24	15.38	15.36	15	15.18	14.86
16	15.63	15.75	15.71	15.62	15.63	15.97	15.89	16.24	16.38	16.36	16	16.18	15.95
17	16.63	16.75	16.71	16.62	16.63	16.97	16.89	17.24	17.38	17.36	17	17.18	16.95

angle for the month of November is equal to the latitude. For this month, a solar collector tilted at an angle equal to the latitude will receive solar radiation normally. Indeed, for the other months, photovoltaic modules need a

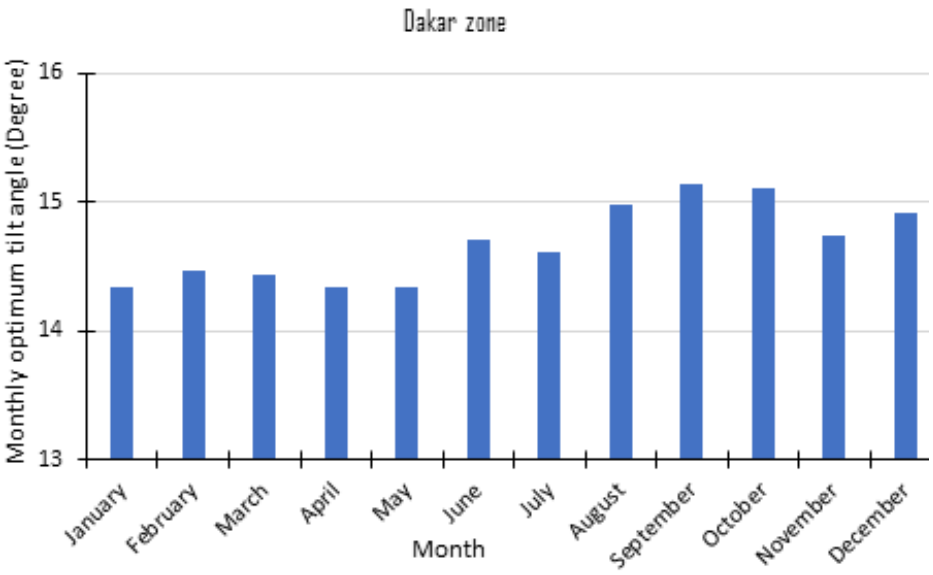

Figure 6. The variation of monthly optimum tilt angle β_(opt,m) for Dakar zone.

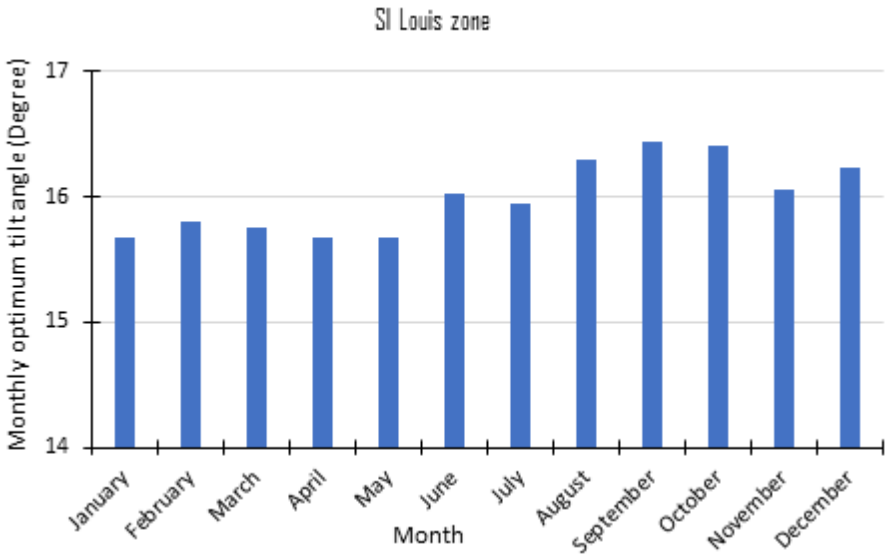

Figure 7. The variation of monthly optimum tilt angle β_(opt,m) for St Louis zone.

monthly adjustment to produce a maximum of electricity. As a result, energy losses will occur if we take the latitude throughout the year.

Application for four typical climatic zones for monthly optimum tilt angle

The $\beta_{opt,m}$ variation for the four typical climatic zones of Senegal is plotted in Figures 6, 7, 8 and 9. For these different zones too, only the month of November gives angle values equal to the latitude. We noticed that the optimum tilt angle varies from one month to another and also from zone to zone.

Figure 6 shows the results of the monthly variation of the optimum tilt angle at Dakar. There is a difference of 5.29% between the maximum and minimum values of the optimum tilt angle. Between the latitude and the minimum of the optimum tilt angle this difference is 2.71%. The variance is 2.64% between the maximum of the optimum tilt angle and the latitude.

At St Louis the results of the monthly variation of the

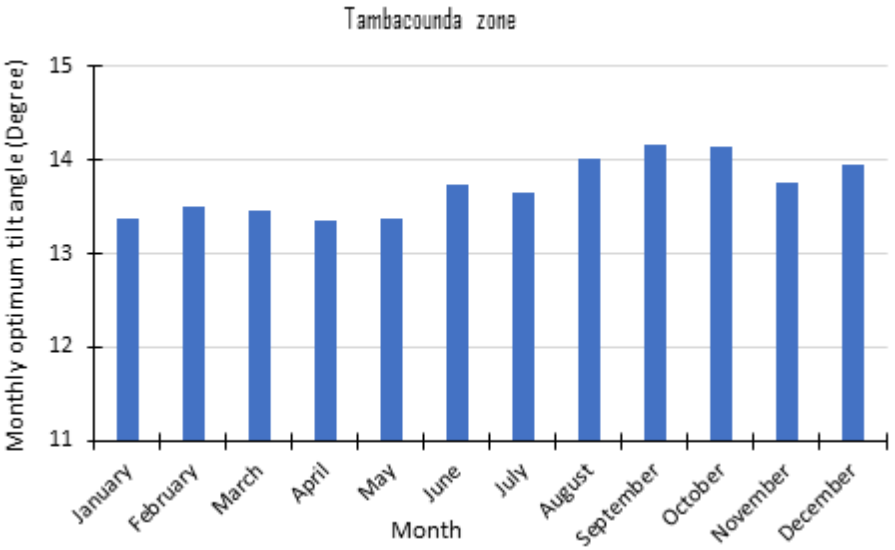

Figure 8. The variation of monthly optimum tilt angle β_(opt,m) for Tambacounda zone.

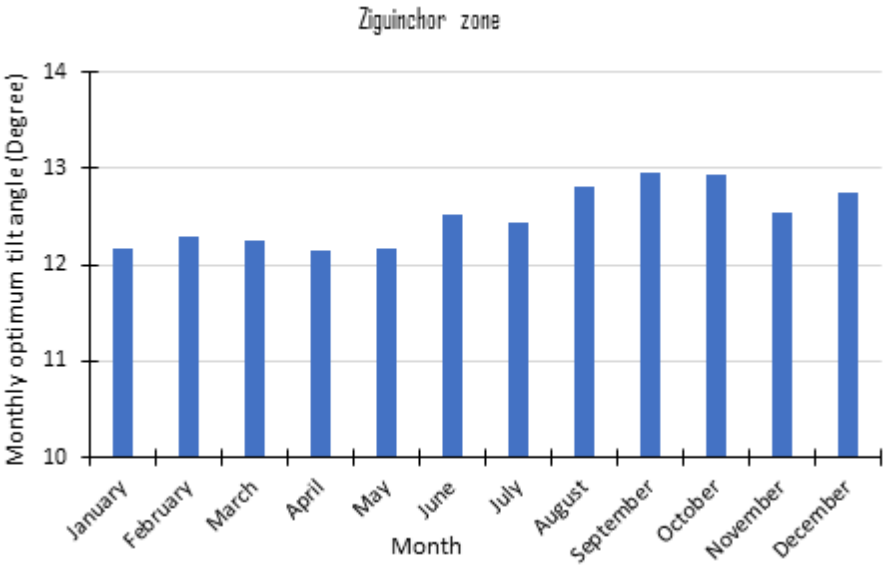

Figure 9. The variation of monthly optimum tilt angle β_(opt,m) for Ziguinchor zone.

optimum tilt angle are presented in Figure 7. The variance between the maximum and minimum values of the optimum tilt angle is 4.64%. The variance between the latitude and minimum of the optimum tilt angle is 2.37%. The variance between the maximum of the optimum tilt angle and the latitude is 2.32%.

In Tambacounda (Figure 8), the monthly variation between the maximum and minimum values of the optimum tilt angle is 5.68%. In fact, this difference represents 2.93% between latitude and the minimum of the optimum tilt angle, while it is 2.84% between the maximum of the optimum tilt angle and latitude.

In the Ziguinchor area (Figure 9), there is a monthly variation of 6.14% between the maximum and minimum values of the optimum tilt angle. However, between the latitude and the minimum of the optimum tilt angle the difference is 3.17% while it is 3.07% between the maximum of the optimum tilt angle and the latitude.

Conclusion

The optimum tilt angle plays an important role in improving the energy collection of solar collectors. In this

study, the optimum values of tilt angles for solar collectors in Senegal were determined using a mathematical model. The results showed a daily variation of the tilt angle of 20.05% in Dakar, 18.74% in St Louis, 23.43% in Tambacounda and 23.01% in Ziguinchor. On the other hand, the monthly variation of the optimum tilt angle is 5.29% in Dakar, 4.64% in St Louis, 5.68% in Tambacounda and 6.14% in Ziguinchor. The annual optimum tilt angle is approximately equal to the latitude of the location. Comparing these four climatic zones, we note that the variation is less important in St Louis and Dakar than in Ziguinchor and Tambacounda. The best orientation for solar collectors in Senegal is due south. To increase the efficiency of solar collector use, it is recommended, if possible, to mount the solar collector at the average monthly tilt angle and adjust the tilt once a month, as indicated by this study.

CONFLICTS OF INTEREST

The authors have not declared any conflict of interest.

ACKNOWLEDGEMENTS

The authors gratefully acknowledge the financial support of CRDI (Centre de Recherches pour le Développement International) and MERIDIAM through the project “Projet d'appui à la filière photovoltaïque par la formation, la recherche et le soutien aux entreprises”.

REFERENCES

Ayaz R, Durusu A, Akca H (2017). Determination of Optimum Tilt Angle for Different PV Technologies Considering Ambient Conditions: A Case Study for Burdur, Turkey. Journal of Solar Energy Engineering 139(4):1-32.

Bakirci K (2012). General models for optimum tilt angles of solar panels: Turkey case study. Renewable and Sustainable Energy Reviews 16(8):6149-6159.

Dixit TV, Yadav A, Gupta S (2017). Annual Optimum Tilt Angle Prediction of Solar Collector using PSO Estimator, IOP Conference Series: Materials Science and Engineering 225:1.

Eke AB (2011). Prediction of optimum angle of inclination for flat plate solar collector in Zaria, Nigeria. Agricultural Engineering International: CIGR Journal 13:4.

El-Kassaby MM (1988). Monthly and daily optimum tilt angle for south facing solar collectors; theoretical model, experimental and empirical correlations. Solar and Wind Technology 5(6):589-596.

Fadaeenejad M, Mohd Radzi MA, Fadaeenejad M, Zarif M, Gandomi Z (2015). Optimization and comparison analysis for application of PV panels in three villages. Energy Science and Engineering 3(2):145-152.

Hailu G, Fung AS (2019). Optimum tilt angle and orientation of photovoltaic thermal system for application in Greater Toronto Area, Canada. Sustainability (Switzerland) 11:22.

Handoyo EA, Ichsani D, Prabowo (2013). The optimal tilt angle of a solar collector. Energy Procedia 32:166-175.

Hartner M, Ortner A, Hiesl A, Haas R (2015). East to west - The optimal tilt angle and orientation of photovoltaic panels from an electricity system perspective. Applied Energy 160:94-107.

Hussein HMS, Ahmad GE, Mohamad MA (2000). Optimization of operational and design parameters of plane reflector-tilted flat plate solar collector systems. Energy 25(6):529-542.

Idowu OS, Olarenwaju OM, Ifedayo OI (2013). Determination of optimum tilt angles for solar collectors in low-latitude tropical region. International Journal of Energy and Environmental Engineering 4(1):1-10.

Ihaddadene N, Ihaddadene R, Charik A (2017). Best Tilt Angle of Fixed Solar Conversion Systems at M’Sila Region (Algeria). Energy Procedia118:63-71.

Kacira M, Simsek M, Babur Y (2004). Determining optimum tilt angles and orientations of photovoltaic panels in Sanliurfa, Turkey 29(8):1265-1275.

Kamanga B, Kamunda C, Mlatho JS, Mikeka C (2014). Optimum Tilt Angle for Photovoltaic Solar Panels in Zomba District, Malawi. Journal of Solar Energy pp. 1-9.

Khahro SF, Tabbassum K, Talpur S, Alvi MB, Liao X, Dong L (2015). Evaluation of solar energy resources by establishing empirical models for diffuse solar radiation on tilted surface and analysis for optimum tilt angle for a prospective location in southern region of Sindh, Pakistan. International Journal of Electrical Power and Energy Systems 64:1073-1080.

Lewis G (1987). Optimum tilt of a solar collector. Solar and Wind Technology 4(3):407-410.

Li DHW, Lam TNT (2007). Determining the Optimum Tilt Angle and Orientation for Solar Energy Collection Based on Measured Solar Radiance Data. doi: 10.1155/2007/85402.

Lv Y, Si P, Rong X, Yan J, Feng Y, Zhu X (2018). Determination of optimum tilt angle and orientation for solar collectors based on effective solar heat collection. Applied Energy 219:11-19.

Mahdi EJ, Abdul-wahid N, Shakerabdulstar S (2011) ‘Güneş Panelini Optimum Konumlandırmak 37:3.

Mehleri ED, Zervas PL, Sarimveis H, Palyvos JA, Markatos NC (2010). Determination of the optimal tilt angle and orientation for olar photovoltaic arrays. Renewable Energy 35(11):2468-2475.

Moghadam H, Tabrizi FF, Sharak AZ (2011). Optimization of solar flat collector inclination. Desalination 265(1-3):107-111.

Mahmoud M, Nabhan I (1990). Determination of optimum tilt angle of single and multi rows of photovoltaic. Solar & Wind Technology 7(6):739-745.

Saraf GR, Hamad FAW (1988). Optimum tilt angle for a flat plate solar collector. Energy Conversion and Management 28(2):185-191.

Sarr A, Kebe CM, Ghennioui A (2020a). Comparative approach for global solar estimation in four typical Senegalese climatic zones. 2020 5th International Conference on Renewable Energies for Developing Countries, REDEC 2020. 5:1-6.

Sarr A, Kebe CM, Ndiaye A (2020a). Analysis and feasibility of 50 kWp self-consumption solar photovoltaic system for four Senegalese typical climatic zones using PVsyst software. International Journal of Physical Sciences 15(4): 201-212.

Shariah A, Al-Akhras MA, Al-Omari IA (2002). Optimizing the tilt angle of solar collectors. Renewable Energy 26(4):587-598.

Skeiker K (2009). Optimum tilt angle and orientation for solar collectors in Syria. Energy Conversion and Management 50(9):2439-2448.

Yadav S, Hachem-Vermette C, Panda SK, Tiwari GN, Mohapatra SS (2021). Determination of optimum tilt and azimuth angle of BiSPVT system along with its performance due to shadow of adjacent buildings. Solar Energy 215:206-219.

Stanciu D, Stanciu C, Paraschiv I (2016). Mathematical links between optimum solar collector tilts in isotropic sky for intercepting maximum solar irradiance. Journal of Atmospheric and Solar-Terrestrial Physics 137: 58-65.

Tiris M, Tiris C (1998). Optimum collector slope and model evaluation: Case study for Gebze, Turkey. Energy Conversion and Management 39(3-4):167-172.

Tripathy M, Yadav S, Sadhu PK, Panda SK (2017). Determination of optimum tilt angle and accurate insolation of BIPV panel influenced by adverse effect of shadow. Renewable Energy104:211-223.

Zang H, Guo M, Wei Z, Sun G (2016). Determination of the Optimal Tilt Angle of Solar Collectors for Different Climates of China pp. 1-16.

Vol. 15(6), pp. 223-229, June 2021
DOI: 10.5897/AJEST2020.2888
Article Number: 99469D467002
ISSN: 1996-0786

http://www.academicjournals.org/AJEST

ACADEMIC JOURNALS
expand your knowledge

African Journal of Environmental Science and Technology

Full Length Research Paper

Diversity of arbuscular mycorrhizal fungi associated to Sorghum (*Sorghum bicolor* L. Moench) in soils of Sikasso region (Mali)

Souleymane KONÉ* and Fallaye KANTÉ

Laboratory of Soil Microbiology, Department of teaching and Research of Biology, Faculty of Sciences and Techniques, University of Sciences, Techniques and Technologies of Bamako (USTTB), Mali.

Received 16 July, 2020; Accepted 15 January, 2021

In Mali, studies on arbuscular mycorrhizal fungi (AMF) characterization and diversity are still few, despite the important roles played by these microorganisms in plant growth and in degraded soils restoration. Sorghum is one of the staple food grains in Mali and as such plays a key role in food security in Mali. This study aims to determine diversity of AMF strains associated to sorghum in Sikasso region soils in Mali. For this, soils were sampled using sorghum plants in different fields of this region, which served as substrates for trapping AMF. These soils have been studied separately. Results gotten revealed 21 AMF morphotypes left between 6 genera (*Glomus*, *Scutellospora*, *Gigaspora*, *Acaulospora*, *Entrophospora*, *Sclerocystis*) of three families (*Glomeracea*, *Gigasporacea, Scutellosporacea*). Four of these morphotypes have been identified.

Key words: Diversity, arbuscular mycorrhizal fungi (AMF), Sikasso, Mali.

INTRODUCTION

In Sub-Saharan Africa, climatic changes associated with anthropogenic pressure, have led to disappearance of woody plant cover. This degradation seriously affects diversity and abundance of symbiotic soil microflora (Diouf and Sougoufara, 2002). However, these symbiotic microorganisms play a fundamental role in soil fertility restoration and maintenance, in protection against certain telluric pathogens and in mineral nutrition of plants. In this area, mycorrhizal fungi, especially those with arbuscular mycorrhizal fungi (AMF), have been shown to be effective. AMF are naturally present in soils of natural ecosystems or agro-ecosystems (Oehl et al., 2004) and has established a compulsory symbiosis with more than 200.000 cultivated plants (Smith and Read, 2008). They have been widely described in tropics (Lambers et al., 2006) and have improved plant growth by better removal and transfer of nutrients, especially phosphorus (Finlay, 2008). Phosphorus is one of the most important elements that significantly affect plants growth and functioning and can represent up to 0.2% of its dry weight (Smith et al., 2011).

The decrease in soil fertility and consequently that in sorghum yields 0.2 to 1.1 tons per hectare in the Sahelian zone could be optimized to 3 or even 4 tons with fertilization (Vaksmann et al., 2008; Dembélé et al., 2011). Inoculation of plants with performing strains AMF

*Corresponding author. E-mail: souleymanekone65@yahoo.fr. Tel: (00223) 76378956.

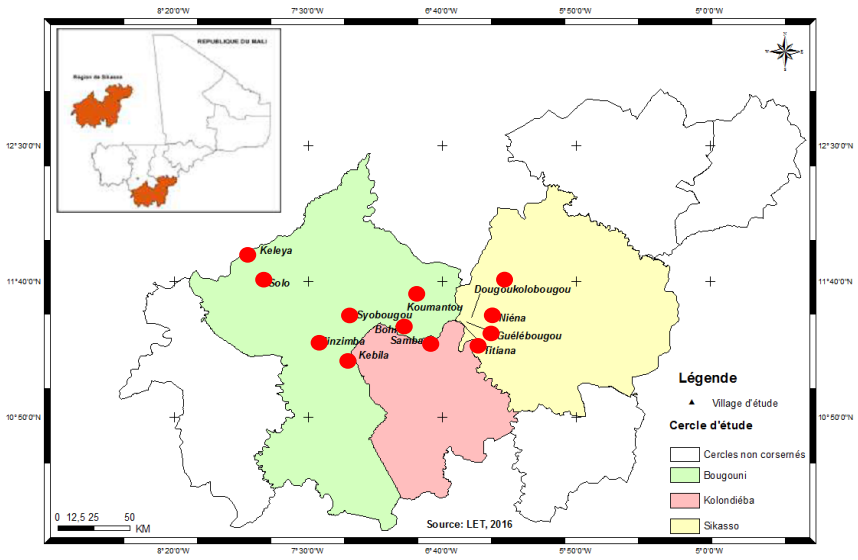

Figure 1. Location of study sites in Sikasso region.
Scale: 1 / 300,000,000

(Fitter, 2012) has been considered to increase plant yield and reduce the use of chemical fertilizers that pollute the environment (Mummey et al., 2009).

In Mali, studies driven on AMF characterization and diversity remains scarcely used for microbial ecology. To our knowledge, the first investigations in this area were carried out in a study in the Sudanian zone in Mali on the positive influence of the age of fallow where the total number of mycorrhizal spores per unit of soil was noted (Sidibé and Yossi, 1997). However, it must be recognized that these fungi biology is complex and their identification represents a challenge for plant symbiosis. Despite this, knowledge accumulated in morphology and anatomy terms would allow a variety of AMF to be identified.

In the country, sorghum is one of the staple food grains in Mali (Bazile et al., 2004). These cereals occupy 75% of cultivated areas and the share of sorghum in the production of dry cereals, which mobilizes around 80% of rural populations, was 35% in 2003 (CILSS, 2002; Sarr, 2010). Moreover, Mali is the second country in the world to meet most of its food needs with sorghum and millet (Bazile et al., 2008). The objective this study was to determine diversity of AMF strains associated to sorghum in Sikasso region soils, Mali.

MATERIALS AND METHODS

Study area

The study was conducted in Sikasso region, located in extreme south of Mali between 12°30 ′ north latitude and 8°45 ′ west longitudes. It covers an area of 71790 km^2 or 5.8% of national territory. It has 7 circles (Sikasso, Bougouni, Kadiolo, Kolondieba, Koutiala, Yanfolila, Yorosso), 3 urban communes (Sikasso, Bougouni, Koutiala), 144 rural communes, including Kolondieba and 1831 villages. An average annual temperature of 27°C is observed between April and May and an average of 24°C between December and January. These sites belong to the humid Sudanian zone in the North between the 750 mm isohyets in the North and 1150 mm in the South and the Guinean zone between the 1150 mm isohyets in the North and 1400 mm in the South (CSA., 2007) and the soil fertility leached tropical ferruginous soils, eroded ferralitic soils and mineral hydromorphic soils in lowlands (MATCL., 2012). This makes the region "the granary" of the country. Agricultural productions are indeed important, such as cereals and fruits (notably mangos). Cotton, which is the 1st export product of the country, is chiefly developed (National Institute of Statistics, 2010).

Study sites

The study comprises 12 sites: Keleya, Solo, Koumantou, Chobougou in Bougouni circle, Sinsimba, Boye, Kébila, Samba in Kolondièba circle, Guélébougoula, Dougoukolobougou, Titiéna and Niéna in Sikasso circle (Figure 1).

Soil sampling

At each site, 1 kg of soil was sampled during the dry season of 2014 at eight different points in surface horizons (0 to 30 cm), with an auger of 5 cm diameter in a sorghum field and a composite soil sample was constituted for each field. The composite samples have been put in bags and these bags were labeled, and then taken to the laboratory.

Trapping of arbuscular mycorrhizal fungal under sorghum plants

Trapping method (Walker, 1992) was used for the AMF diversity study in the different sites. It consisted of growing sorghum in polyethylene pots of 2.23 cm^3, previously washed and disinfected

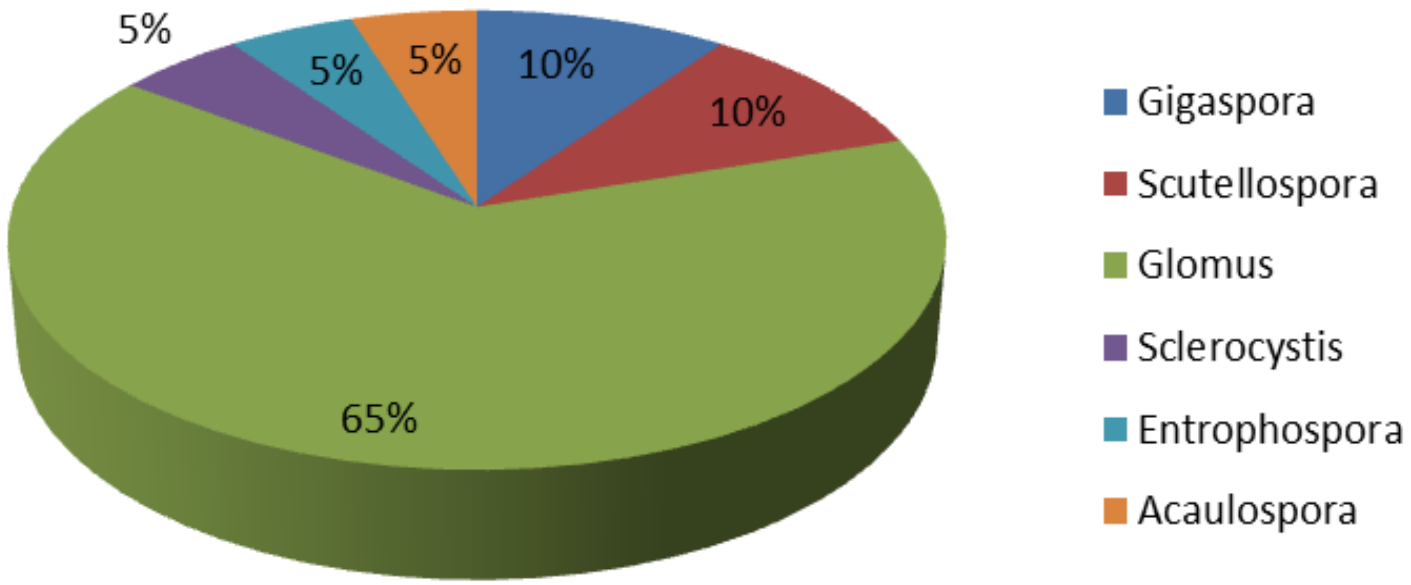

Figure 2. Relative abundance of spores on different genera of AMF isolated after trapping in greenhouse on sorghum cultivation soils.

with bleach, containing 2.1 kg of growing medium. Work has been done in greenhouse with one day/night temperature: 30°/25°C, photoperiod: 16 h. Three sorghum seeds were sown in each pot. Three pots have been considered by soil, making a total of thirty six pots. Plantations were daily watered with demineralized water at field capacity (14%, vol/weight). After 4 months cultivation, culture soils were removed for determination of AMF diversity.

Spore extraction

It was carried out according to wet sieving method described by Gerdemann and Nicholson (1963). It involved a sample of 100 g dry soil. Four repetitions have been considered for each soil.

Morpho-anatomical characterization of AMF spores

The morphology of the spores is the basis of their identification. For that, spores size, shape and color, their solitary or grouped nature, their clusters dissociable nature or not, presence or absence of sporogenic cell on spores were noted by discriminating spores extracted from each soil under microscopic. Data obtained were compared with original description by Schenck and Pérez (1990) and that of database of reference cultures published on the website (http: //invam.caf.wvu.edu, August 2016).

Preparation of the blades

Spores morphologically identical were removed using a pipette and then placed on a microscope slide containing each of these ends on a drop of distilled water. Two drops of PVLG solvent (polyvinyl alcohol, lactic acid, glycerol) (Koske and Testier, 1983) were placed at right end of the slide to allow observation of spore external morphology. Two drops of PVLG + Melzer v/v reagent (Morton, 1988) were placed at the left end to study membrane layers. At each end of slide containing drops of solvent, one to several similar spores were deposited and then gently covered with a coverslip.

Microscopic observation of spores

Spores were observed under an optical microscope with enlargement 10 (G X 10). After observing external morphology, using forceps, a pressure was gently applied above coverslip, covering PVLG solvent added to Melzer reagent pending bursting spores. Owing to the solvents, internal membranes of spores emerged after rupture.

RESULTS

Extracted AMF community structures

AMF spores morphology and anatomy observation enabled identification of 21 morphotypes for all 12 sites (Figure 2). These morphotypes belong respectively to six genera, *Gigaspora*, *Scutellospora*, *Glomus*, *Sclerocystis*, *Entrophospora* and *Acaulospora;* distributed in three families namely *Gigasporaceae*, *Glomeraceae*, and *Acaulosporaceae*. The comparison with the genera composition and the relative abundances of these genera in soils collected directly from the field shows the same genera composition in the soils before and after trapping. The structure of the different AMF communities also remains quite similar (Figure 3).

Relative abundance of different morphotypes from trapping soil

Glomus genus is most represented and most diversified with 15 morphotypes (65% of species observed). One of this genus morphotypes was identified using these

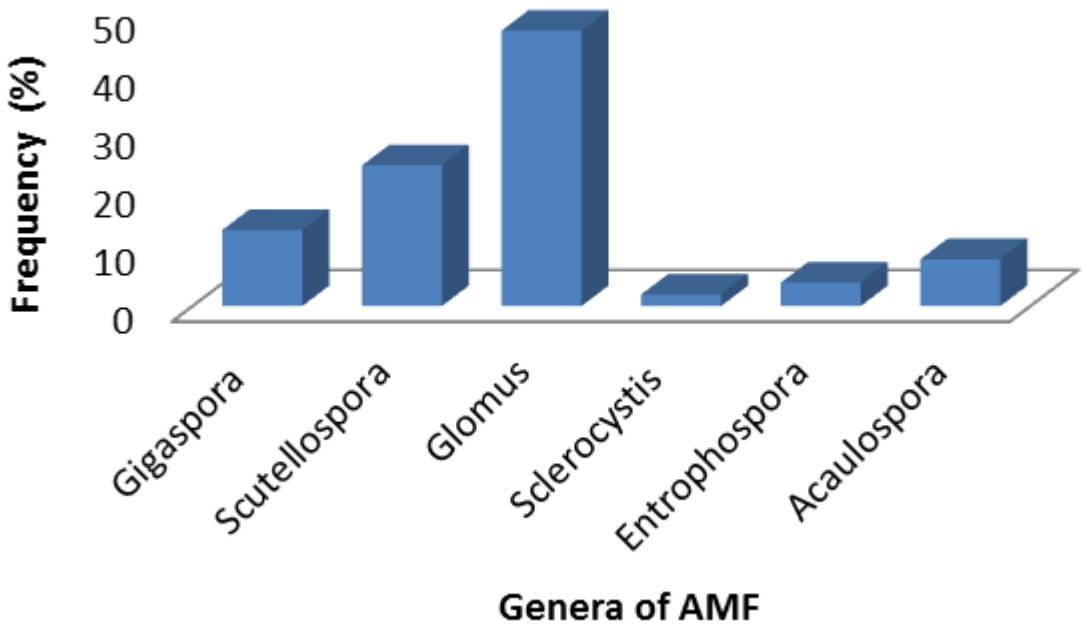

Figure 3. Relative abundance of spores on different genera of AMF associated with sorghum at study sites.

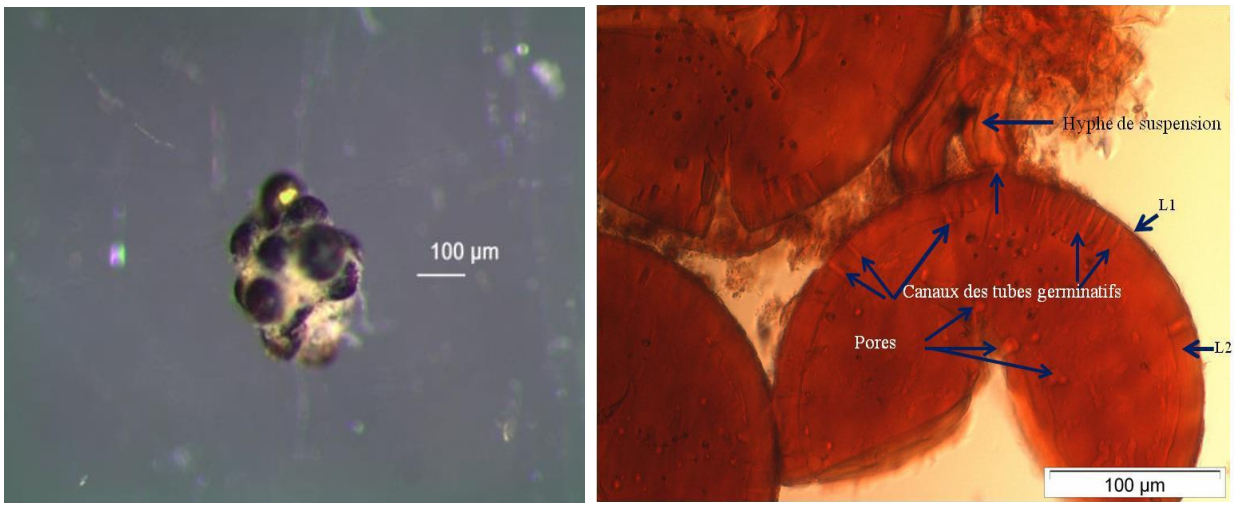

Figure 4. Morphology (a) and membrane structure (b) of *Glomus coronatum* spores.

morpho-anatomical characters as *Glomus coronatum* (Figure 4a and b), and the other fourteen unidentified were named *Glomus spp.* These are *Glomus* spp1 to *Glomus* spp14. The genera *Scutellospora* and *Gigaspora* are each represented by two morphotypes, 10% of each species were obtained. Two species of *Scutellospora* genus have been identified on account of their morpho-anatomical characters as *Scutellospora gregaria* and *Scutellospora heterogama* (Figure 5a, b and 6a, b). The morpho-anatomical characters of *Gigaspora* genus identified one of the two morphotype like *Gigaspora rosea* (Figure 7a and b). The other unidentified morphotype was named *Gigaspora* sp. *Acaulospora*, *Entrophospora* and *Sclerocystis* generas; each represented by a single morphotype or 5% of species. These generas have been respectively named *Acaulospora* sp., E*ntrophospora* sp. and *Sclerocystis* sp.

DISCUSSION

This study showed a diversity of AMF associated with

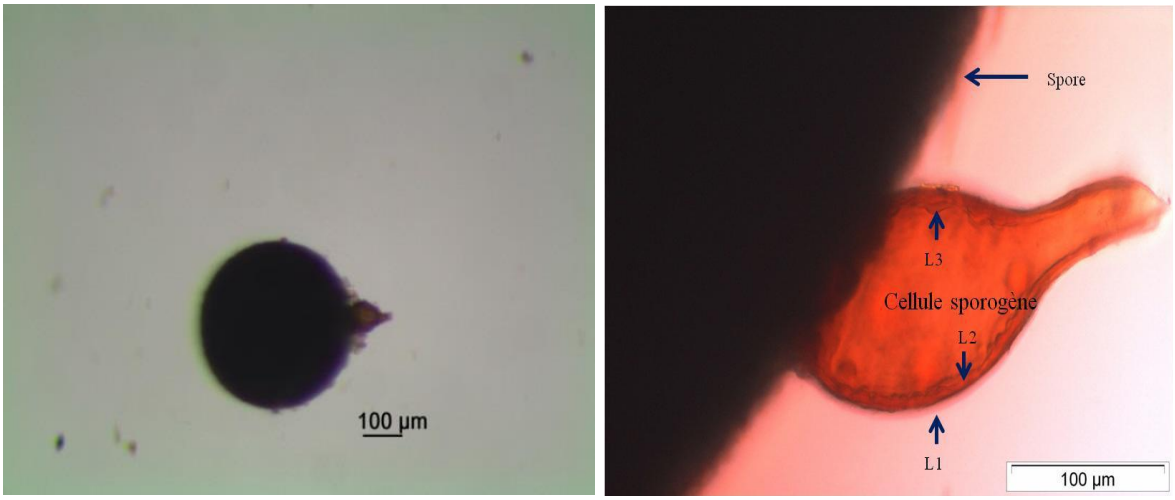

Figure 5. Morphology (a) and membrane structure (b) of *Scutellospora gregaria* spores.

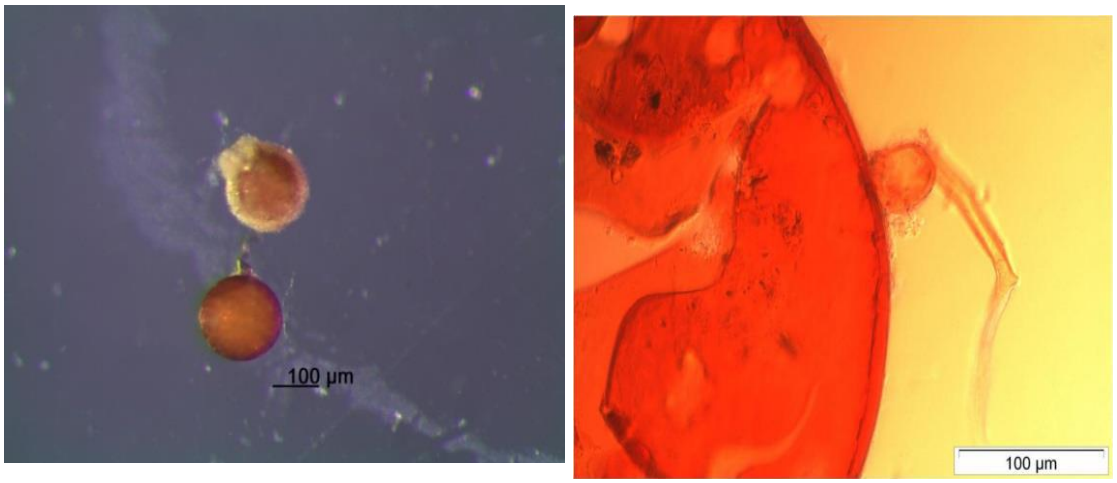

Figure 6. Morphology (a) and membrane structure (b) of *Scutellospora heterogama* spores.

sorghum in the 12 soils of Sikasso in Mali. The genus *Glomus* is the most represented in all sites with 15 morphotypes (65%). Such a result has been noted in different natural and agro-ecological environments in West Africa as well as in Ivory Coast (Anguiby et al., 2019), in Togo (Gnamkoulamba et al., 2018), in Benin (Aguegue et al., 2017), in Senegal (Diop et al., 2015), and in India (Ajaz et al., 2017). Indeed, it has been reported that the genus *Glomus* predominates in terms of presence in ecosystems due to its adaptability and stability in tropical environments and various conditions (Lenoir et al., 2016b; Bencherif et al., 2015).

Spores are differentiated in the soil and in the roots (case of the genus Sclerocystis). They are used as a reference structure for the morpho-anatomical identification of species. These spores are generally round in shape, with a thick wall formed of several layers of different textures and connected to the filamentous network by a suspensory hypha.

The diversity observed in present study, comprising 21 morphotypes of 6 genera (*Glomus*, *Gigaspora*, *Scutellospora*, *Acaulospora*, *Rhyzophagus* and *Entrophosphora*) is greater than that of four genera (*Glomus*, *Gigaspora*, *Scutellospora*, and *Acaulospora*) obtained under the Cheese and Makorés in a Botanical garden in Ivory Coast (Anguiby et al., 2019) from 10 specimens, but lower than that of seven genera (*Acaulospora*, *Claroideoglomus*, *Entrophospora*, *Funneliformis*, *Gigaspora*, *Glomus* and *Rhizoglomus*) observed under different rice cropping systems in Togo (Gnamkoulamba et al., 2018) which brought in 25 species. With 15 morphotypes (Diop et al., 2015) also

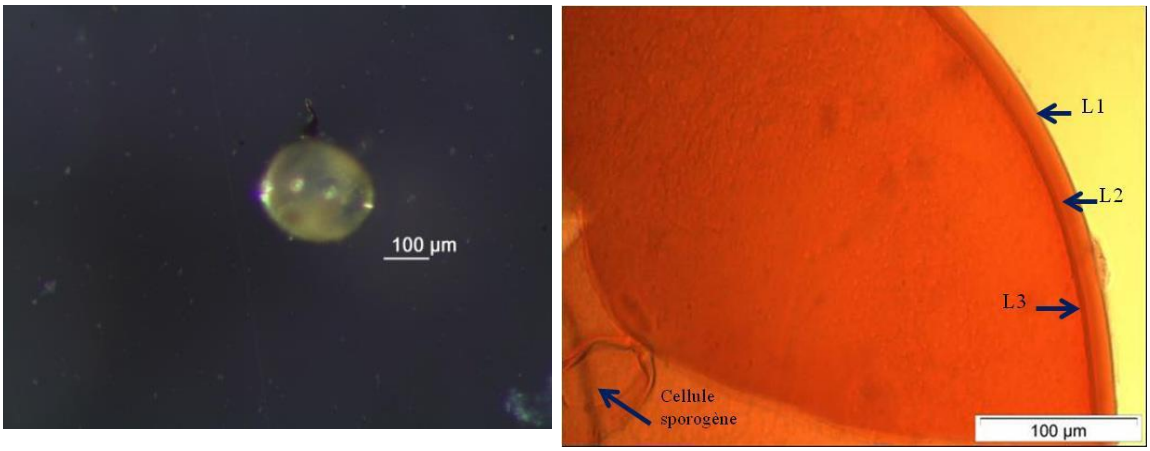

Figure 7. Morphology (a) and membrane structure (b) of *Gigaspora rosea* spores.

obtained in Senegal. These results are consistent with those of other authors regarding the existence of a diversity of AMF in soils of agro systems in West Africa. Indeed, the African west soils contain a big/great diversity AMF that can be identified, thanks to the morphology of their spores (Dalpé et al., 2000). In addition, these fungi are subservient to plants and do not exhibit host specificity; hence the diversity observed here in Mali and elsewhere in Sub-Saharan Africa.

Conclusion

In the Sikasso region of Mali, sorghum is naturally associated with a great diversity of arbuscular mycorrhizal fungi, identified in 21 morphotypes from six genera and three families. The genus *Glomus* was the most represented and diverse with fifteen morphotypes. Further work can be done by sequencing the strains in the collection.

CONFLICT OF INTERESTS

The authors have not declared any conflict of interests.

REFERENCES

Aguegue RM, Noumavo PA, Gustave, Dagbenonbakin D, Baba Moussa L (2017). Arbuscular Mycorrhizal Fertilization of Corn (*Zea mays* L.) Cultivated on Ferrous Soil in Southern Benin. Journal of Agricultural Studies 5(3):99-115.

Ajaz M, Mohammad YZ, Jagana CS (2017). Isolation, Identification and Characterization of Arbuscular Mycorrhizal Fungi in Apple (Malus Domestica Borkh) Growing Area of Kashmir Himalaya". International Journal of Current Microbiology and Applied Sciences 6(8):25-37.

Anguiby BLA, Ouattara G, Bomisso EL, N'goran B, Ouattara B, Coulibaly SA, Aké S (2019). Assessment of the mycorrhizal status of trees of *Ceiba pentandra* (L), Gaertn and *Tieghemella heckelii* (A.Chev), Pierre, from the Botanical Garden of Bingerville in Ivory Coast. Journal of Applied Biosciences 138:14092-14105.

Bazile D, Dembélé S, Soumaré M, Dembélé D (2008). Use of the varietal diversity of sorghum to enhance the diversity of soils in Mali. Cahiers Agricultures vol. 17, n°2, Cirad/IER, Bamako / Mali.

Bazile D, Soumaré M, Dembélé J (2004). Sorghum in Mali: Conserving agro-biodiversity for the stability of agricultural production. Sub-regional workshop on agricultural biodiversity in West Africa, December 15 to 19. GTZ / FAO, Bamako, Mali. Technical Sheet, Sorghum Program/CRRA/Sotuba-IER.16 p.

Bencherif K, Boutekrabt A, Fontaine J, Laruelle, F, Dalpè Y, Lounès-Hadj Sahraoui A (2015). Impact of soil salinity on arbuscular mycorrhizal fungi biodiversity and microflora biomass associated with *Tamarix articulata* Vahll rhizosphere in arid and semi-arid Algerian areas. Science of the Total Environment 533:488-494.

Commission of Food Safety (CSA) (2007): Summary of municipal food security plans in the Sikasso region. PROMISAM /USAID-Mali 19p.

Dalpé Y, Diop TA, Plenchette C, Guèye M (2000). Glomales species associated with surface and deeprhizosphere of *Faidherbia albida* in Senegal. Mycorrhiza 10:125-129.

Dembélé B, Diourté M, Traoré H, Wade M, Mourik TV, Macauley HR, Asiedu E, Koné AY, Kouamé KJ (2011). Promotion of striga-resistant sorghum varieties for the mitigation of food crises in the Senegal, Mali, Ghana and Burkina Faso. Global Food Security Response Initiative. Sorghum seed production training manual. CORAF/ WECARD. Food Crops Program 34:12-16.

Diop I, Ndoye F, Kane A, Krasova-Wade T, Pontiroli A, Do Rego FA, Noba K, Prin Y (2015). *Arbuscular mycorrhizal* fungi (AMF) communities associated with cowpea in two ecological site conditions in Senegal. African Journal of Microbiology Research 9(21):1409-1418.

Diouf D, Sougoufara B (2002). "Reforestation in Senegal: assessment of achievements from 1993 to 1998." Rev. For. Fr. LIV: 227-238.

Finlay RD (2008). Ecological aspects of mycorrhizal symbiosis with special emphasis on the functional diversity of interactions involving the extraradical mycelium. Journal of Experimental Botany 59(5):1115-1126.

Fitter A (2012). Why plant science matters. The New Phytologist 193(1):1-2.

Gerdemann JW, Nicholson TH (1963). Spores of mycorrhizal Endogone species extracted from soil by wet sieving and decanting. Transactions of the British Mycological Society 46(2):235-244.

Gnamkoulamba A, Tounou AK, Tchabi A, Agboka K, Adjévi AKM, Batawila K (2018). Prevalence and diversity of spores of arbuscular mycorrhizal fungi in rice cultivation under different rice cropping systems in Togo. Journal of Applied Biosciences 126:12647-12664.

Permanent Interstate Drought Control Committee (CILSS) (2002). Strategic framework for sustainable food security in a perspective of poverty reduction in the Sahel. Niamey (Niger) 52:9-10.

Koske RE, Testier B (1983). A convenient, permanent slide mounting medium. Mycological Society of America Newsletter 34(2):59.
Lambers H, Shane MW, Cramer MD, Pearse SJ, Veneklaas J (2006). Root structure and functioning for efficient acquisition of phosphorus: matching morphological and physiological traits. Annals of Botany 98(4):693-713.
Lenoir I, Fontaine J, Lounès-Hadj Sahraoui A (2016b). Arbuscular mycorrhizal fungal responses to abiotic stresses: A review. Phytochemistry 123:4-15.
Ministry of Territorial Administration and Local Authorities (MATCL) (2012). Diagnostic study of promising economic sectors and shared economic spaces in the Sikasso region. GERAD 100 p.
Morton JB (1988). Taxonomy of VA mycorrhizal fungi: Classification, nomenclature and identification. Mycotaxon 32:267-324.
Mummey DL, Antunes PM, Rillig MC (2009). Arbuscular mycorrhizal fungi pre-inoculant identity determines community composition in roots. Soil Biology & Biochemistry 41(6):1173-1179.
National Institute of Statistics (2010). Provisional results of the General Census of Population and Housing.
Oehl F, Sieverding E, Mâder P, Dubois D, Ineichen K, Boller T, Wiemken A (2004). Impact of long-term conventional and organic farming on the diversity of arbuscular mycorrhizal fungi. Oecologia 138(4):574-583.
Sarr MB (2010). Interim report: Baseline study of the agro-food processing system in West Africa. Agri-business and Agro-Food Specialist 53 p.
Schenck NC, Pérez Y (1990). Manual for the Identification of VA Mycorrhizal Fungi. Synergistic-Publications, Gainesville, Florida.
Sidibé DK, Yossi H (1997). Effect of fallow age on the number of endomycorrhizal fungi spores in the Sudanian zone of Mali 1:6-10; Fallow Project. Forest Resources Program; IER; Bamako-Mali.
Smith SE, Jakobsen I, Grønlund M, Smith FA (2011). Roles of *Arbuscular mycorrhizas* in Plant Phosphorus Nutrition: Interactions between Pathways of Phosphorus Uptake in Arbuscular Mycorrhizal Roots Have Important Implications for Understanding and Manipulating Plant Phosphorus Acquisition. Plant Physiology 156(3):1050-1057.
Smith SE, Read DJ (2008). Mycorrhizal symbiosis, 3rd edn. Academic Press Inc., London, 3rd eds.
Vaksmann M, Kouressy M, Chantereau J, Bazile D, Sagnard F, Touré A, Sanogo O, Diawara G, Dante A (2008). Use of the genetic diversity of local sorghums in Mali. Cahiers Agricultures 17:2, Cirad/IER, Bamako/Mali.
Walker C (1992). Systematics and taxonomy of the *Arbuscular endomycorrhizal* fungi (Glomales)- a possible way forward Agronomy 12(10):887-897.

Vol. 15(6), pp. 230-242, June 2021
DOI: 10.5897/AJEST2021.2989
Article Number: 2DF9A4F67018
ISSN: 1996-0786

http://www.academicjournals.org/AJEST

ACADEMIC JOURNALS
expand your knowledge

African Journal of Environmental Science and Technology

Review

CREST/EF5 capacity building to enhance resilience to hydrodynamic disasters in emerging regions

Teshome L. Yami[1*], Shang Gao[1], Mengye Chen[1], Zhi Li[1], Laura Labriola[1], Calvince Wara[2], Feleke Z. Beshah[3] and Yang Hong[1]

[1]Hydrometeorology and Remote Sensing Laboratory, School of Civil Engineering and Environmental Science, University of Oklahoma, Norman, OK 73072, USA.
[2]Regional Center for Mapping of Resources for Development (RCMRD), Nairobi, Kenya.
[3]College of Natural Sciences, Department of Chemistry, Addis Ababa University, Ethiopia.

Received 9 February, 2021; Accepted 19 May, 2021

Water and water-related disasters, e.g. flooding, landslide and droughts, are affecting the world and it is important for decision makers and experts to build the capacity of forecasting hydrodynamic disasters and safeguarding people's life and property. This study focuses on building capacity of decision makers and analysts with an aim to create and support a robust framework for decision makers in integrated water resource management. Capacity building training workshops has been conducted using Coupled Routing and Excess Storage (CREST) and Ensemble Framework for Flash Flood Forecasting (EF5) distributed hydrological modeling jointly developed by University of Oklahoma (OU) and National Aeronautics and Space Administration (NASA), involving Regional Center for Mapping of Resources for Development (RCMRD), ICPAC and Kenyan Meteorological department (KMD). The OU_Applied Science Team (AST) in collaboration with RCMRD provided an EF5 hydrologic model website to KMD to visualize and forecast streamflow. Further, an advanced EF5 training was conducted in East Africa and a system to collect citizen reports to gather observations of flooding was developed. This effort will improve awareness of and access to available services through providing user-tailored services to inform development of decision-making processes and build the capacity of SERVIR hubs and their partners to provide high quality services, creating a stronger network at the regional and international level. The study will guide users/forecasters on how to use EF5 operationally and enhances development of an impact-based flood early warning system with users, linking hydrologic forecasts with vulnerability assessment and risk analysis to mitigate the potential negative impact to the public and properties.

Key words: Capacity building, drought, flood, hydrologic model, landslide, streamflow.

INTRODUCTION

Uganda is at high risk from a variety of hazards, which have the potential to adversely affect progress on poverty reduction and economic growth. Landslides and floods are one of the most important disasters today with floods

alone reported to account for 6.8 million deaths worldwide, estimates indicate that Asia and Africa are among the most vulnerable regions prone to disasters with Asia alone accounting for about 50% of flood related death (Jonkman and Kelman, 2005).

The World Bank has estimated that at least 200,000 Ugandans are affected by disasters each year. The Government of Uganda has identified drought as the most severe disaster affecting the lives and livelihoods of its citizens (Tsarouchi, 2018). Natural disasters can have significant impacts on the health and development of a region. Disasters such as floods, landslides, earthquakes, tropical cyclones, volcanic eruptions, and tsunamis have the potential to be catastrophic and lead to massive alterations in the lives of those affected; effects include loss of property and life, injury and morbidity, long-term displacement, disruptions in livelihoods, and widespread economic effects (Agrawal et al., 2013).

Flooding is another prominent feature of Kampala, frequent high intensity tropical rain storms almost inevitably generate extremely high run-off that quickly exceeds the capacity of the urban storm water drainage system, causing frequent flooding across the city, but especially in the low lying valleys and wetland areas that are typical of Kampala's environment and flooding impacts all socio-economic groups but those urban poor who are occupying the low lying lands and wetlands are most vulnerable (Sliuzas et al., 2013). Therefore knowledge about infiltration capacity in a catchment is extremely important for flooding analyses and common runoff fractions of rural catchments are between 5 and 10% for vegetated surfaces, while urban areas with sealed surfaces can have runoff percentages as high as 30-50%, depending on the soil hydrological properties (permeability and pore space) (Sliuzas et al., 2013).

The occurrence of landslides and floods in East Africa has increased over the past decades with enormous public health implications and massive alterations in the lives of those affected (Resilient Africa Network, 2015). Uganda is one of the African countries most prone to disasters. In 2010, flooding of the banks of river Manafwa and landslides in Bududa district in the Mt. Elgon region left 5,000 individuals displaced and over 400 killed (Atuyambe et al., 2011), the Mt. Elgon region of Uganda is reported to have the highest rates of landslides and floods in the country with devastating effects on the livelihood of people. In the current advent of climate change and the changing environment, it is anticipated that landslide and flood incidents will be on the increase within exposed communities in Mt Elgon region.

Heavy rains in Eastern Uganda precipitated flooding in Butaleja District and landslides Bududa in February and March 2010 (Doocy et al., 2013). The Bududa landslides were among the ten deadliest disasters worldwide in 2010 with 385 deaths and the displacement of over 3,000 people (Center for Epidemiology in Disasters (CRED, 2009); landslides are often triggered by excessive rain in combination with other factors including increased groundwater content, steep slope gradients, land cover, and geologic composition. Landslides are particularly dangerous and often result in high numbers of casualties because of their rapid onset and limited lead-time for evacuation (Dore, 2003; Moe and Pathranarakul, 2006). In the case of the floods in Butaleja, widespread crop and infrastructure damage occurred with more than 33,000 people affected, however, there was little mortality (Butaleja District Government, 2009; UN OCHA, 2010a b). Moreover, floods caused more severe injuries than landslides and resulted in a higher degree of loss of function or disability, Landslides, on the other hand, caused a greater number of fractures and lacerations than floods (Agrawal et al., 2013). In late February of 2010, several consecutive days of heavy rains in the Butaleja and Bududa Districts of Eastern Uganda precipitated flooding and landslides which resulted in the destruction of crops, infrastructure, water and sanitation facilities; widespread displacement; and increased morbidity and mortality (WHO, 2010). However, Government of Uganda (GOU, 2007) indicates that the wetter areas of Uganda, around the Lake Victoria basin and the east and northwest are tending to become wetter, indicating an increase in rainfall in these areas. Temperature and rainfall simulations by Goulden (2008) indicate high percentage increases in rainfall for historically dry seasons for many parts of Uganda.

The Butaleja floods were concentrated in low-lying areas adjacent to the River Manafwa and affected more than 38,780 people (Butaleja District Local Government, 2010) while the Bududa landslides resulted in 388 deaths and was the deadliest disaster in Africa during 2010. (Guha-Sapir, 2010). In the flood-affected District of Butaleja, a sub-county level environmental vulnerability index was created with Geographic Information Systems (GIS) using administrative boundaries from the United Nations, regional rainfall data for the January to May time period, and spatially distributed population data from the Global Rural Urban Mapping Project (GRUMP) (DDGISST, 2010). In the landslide-affected area district of Bududa, a list of most-affected villages was compiled based on the United Nations interagency assessment

*Corresponding author. E-mail: Teshome.L.Yami-1@ou.edu.

report and discussions with the Bulecheke Camp Chairman, Fourteen villages were affected, with six classified as most affected (Agrawal et al., 2013). As a result, clusters assigned to the six most-affected communities were evenly divided between households in communities and those resettled in the camps, the remaining six clusters were assigned to camp residents from the other eight affected villages and the total affected population of each village as reported by the community leader was used to determine the sampling interval for systematic sampling of households (Agrawal et al., 2013). Local level studies conducted in Uganda have been based on the magnitudes of monthly and seasonal rainfall (Kigobe et al., 2011; Komutunga and Musiitwa, 2001) and the occurrence of dry and wet spells (Bamanya, 2007; Osbahr et al., 2011), with limited focus on the variability of rainfall within the year and seasons.

Boko et al. (2007) predict that Africa is likely to warm across all seasons during this century with annual mean surface air temperatures expected to increase between 3 and 4°C by 2099, roughly 1.5 times average global temperatures. Projections in East Africa suggest that increasing temperatures due to climate change will increase rainfall by 5 - 20% from December to February and decrease rainfall by 5-10% from June to August by 2050 (Hulme et al., 2001; IPCC, 2007). Non-governmental organizations working in Uganda also report that farmers recognize an increasingly erratic rainfall pattern in the first March to May rainy season, causing drought and crop failure, but also more intense rainfall, especially in the second rains at the end of the year, causing flooding and erosion (Oxfam, 2008). In comparison, the average long-term annual rainfall for Uganda is 1318 mm, which is considered adequate to support agricultural activities (Osbahr et al., 2011), this implies that Eastern Uganda receives adequate rainfall to support agriculture. Seasonal distribution of rainfall affects the decisions made by farming households on what type of crops to grow and land management practices to adopt (Komutunga and Musiitwa, 2001). In addition, excessive rains both in intensity and duration lead to water logging conditions that negatively affect crops and pasture (GOU, 2007; Komutunga and Musiitwa, 2001). For example, drought in 2008 caused an average reduction in yield of 50% of sorghum, groundnuts, cassava, and maize in Uganda (Ocowunb, 2009).

Floods, despite their slow onset and potential for early warning, are the most significant disaster worldwide in terms of frequency, affected population size, and deaths, in addition to their human impacts, floods damage livelihoods, property and infrastructure resulting and often result in widespread displacement and economic losses (Duclos et al., 1991). Heavy rainfall experienced between 2006 and 2010 is responsible for massive floods in the low land areas and numerous landslides in the mountainous regions in Eastern Uganda (GOU, 2009). This study explored underlying causes and coping strategies used to avert the effects of landslides and floods in Uganda. Therefore, findings on the strategies that have been used to mitigate, to cope positively, recover and learn from the landslides and floods could inform the design of appropriate innovative solutions that can strengthen the capacity of affected populations to become resilient.

History of CREST/EF5 hydrological modeling

To mitigate water and water-related disasters globally, the University of Oklahoma (OU) and the National Aeronautics and Space Administration (NASA) jointly developed the Coupled Routing and Excess Storage (CREST) hydrological model and the Ensemble Framework for Flash Flood Forecasting (EF5) software to run hydrological modeling using NASA data such as precipitation, evapotranspiration from FEWSNET and Stream flows from USGS websites. The EF5 hydrological modeling software was developed using the CREST (Wang et al., 2011) hydrological modeling as a basic source. The CREST model was initially developed to provide real-time regional and global hydrological prediction by running at fine spatiotemporal resolution with maintaining economical computational cost. CREST simulates the spatiotemporal variation of water, energy fluxes and storages on distributed grid cells of arbitrary user defined resolution, which enables multi-scale application. The scalability of CREST simulations is accomplished through the sub-grid scale representation of soil moisture storage capacity (using a variable infiltration curve), multi-scale runoff generation processes (using multi linear reservoirs) and a fully distributed routing scheme (using the fully distributed linear reservoir routing). The primary water fluxes such as infiltration and routing are physically affected by geographic variables land surface characteristics. Table 1 shows CREST distributed hydrological model parameters. The runoff generation and routing components are coupled; therefore, CREST includes more realistic interactions between lower atmospheric boundary layers, terrestrial surface, and subsurface water than another distributed hydrological model. The CREST/EF5 model is forced by gridded evapotranspiration (PET) precipitation datasets that are measured, estimated, and forecasted. The CREST hydrological model and EF5 hydrological model architecture are shown in Figures 1 and 2. The EF5 hydrological modeling software is being updated by Hydrometeorological and Remote Sensing Laboratory (HyDROS) research scientists including reservoir modeling, landslide, and dam to support water

Table 1. CREST distributed hydrological model parameters.

Type	Parameter	Description	Min	Default	Max	Unit
Physical parameter	RainFact	The multiplier on the precipitation field	0.5	1.0	1.2	Mm/day mm
	Ksat	The soil saturated hydraulic conductivity	0	500	3000	
	WM	The Mean Water Capacity	80	120	200	
	B	The exponent of the variable infiltration curve	0.05	0.25	1.5	
	IM	The impervious area ratio	0	0.05	0.2	
	KE	The factor to convert the PET to local actual	0.1	0.95	1.5	
	CoeM	The overland runoff velocity coefficient	1	90	150	

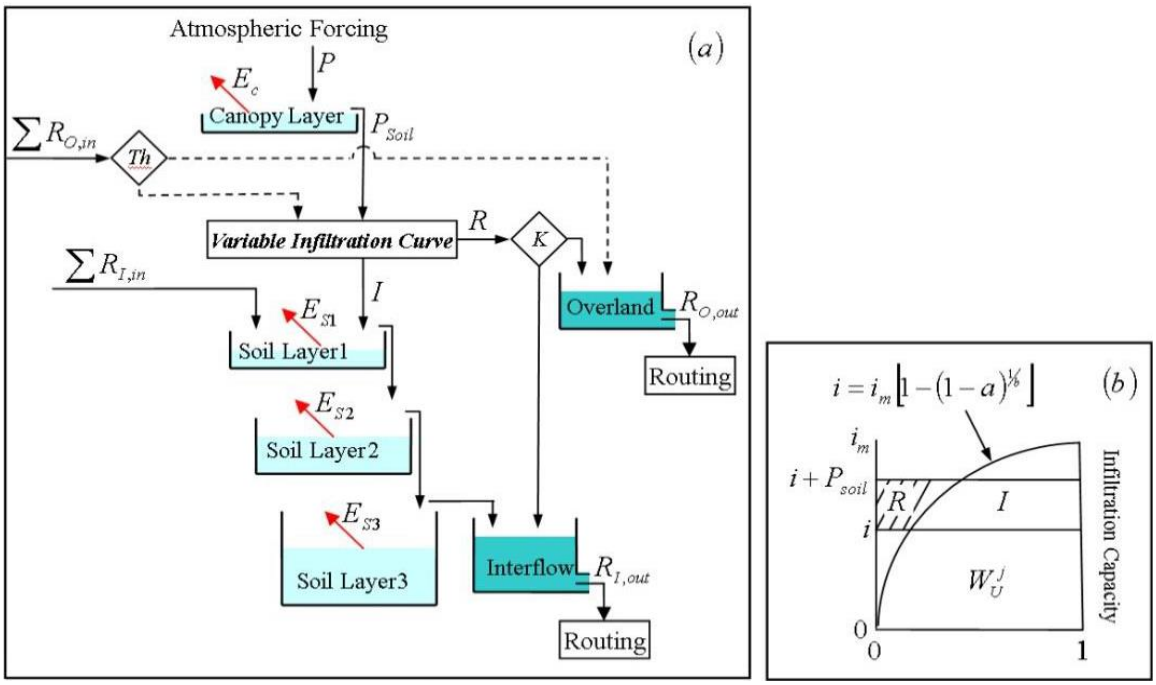

Figure 1. Core Components of the CREST model. The parameters are: Soil saturated hydraulic conductivity (Ksat), Mean water capacity (WM), Impervious area ratio (IM), PET to local actual (KE), Overland runoff velocity coefficient (CoeM).

management works globally (Figure 3).

Regionalized EF5 hydrological modeling in East Africa

A regionalized EF5 Hydrological modeling was developed based on the request from Regional Center for Mapping of Resources for Development (RCMRD) to communicate flood forecasts. Seven Eastern African countries were included in the regionalized hydrological model: Kenya, Uganda, Ethiopia, Rwanda, Tanzania, Burundi, and Malawi (Figure 4). Through several visits and online discussion, the OU Advanced Science Team (AST) has worked with RCMRD, Uganda Ministry of Water and Environment, and Uganda Meteorological Authority to develop a joint plan to expand the current hydrological system coupled with new upgraded modules to Uganda. The Uganda Ministry of Water and Environment has selected the focus areas of intervention in this project; Namatala, Mpologoma and Manafwa river basins (Figure 4) which shows the early results of the CREST/EF5 hydrological modeling conducted on the three basins.

Building upon RCMRD's expertise with the CREST model, EF5 provides several key improvements. First, EF5 can achieve useful results on ungauged basins

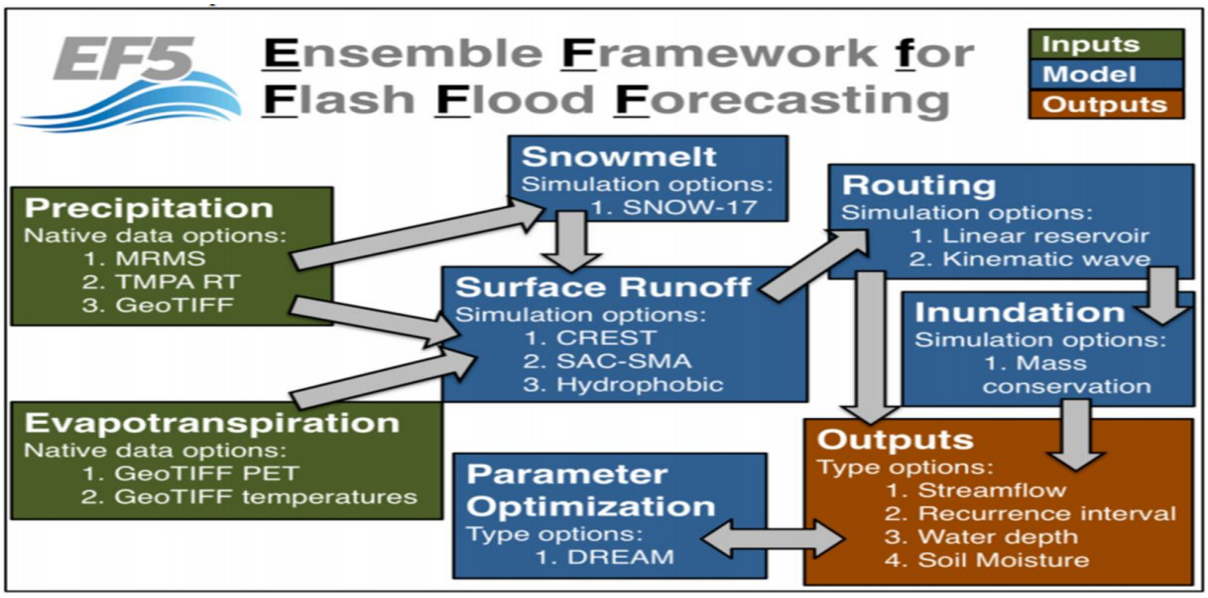

Figure 2. Ensemble Framework for flash flood Forecasting (EF5) Hydrological modeling architecture.

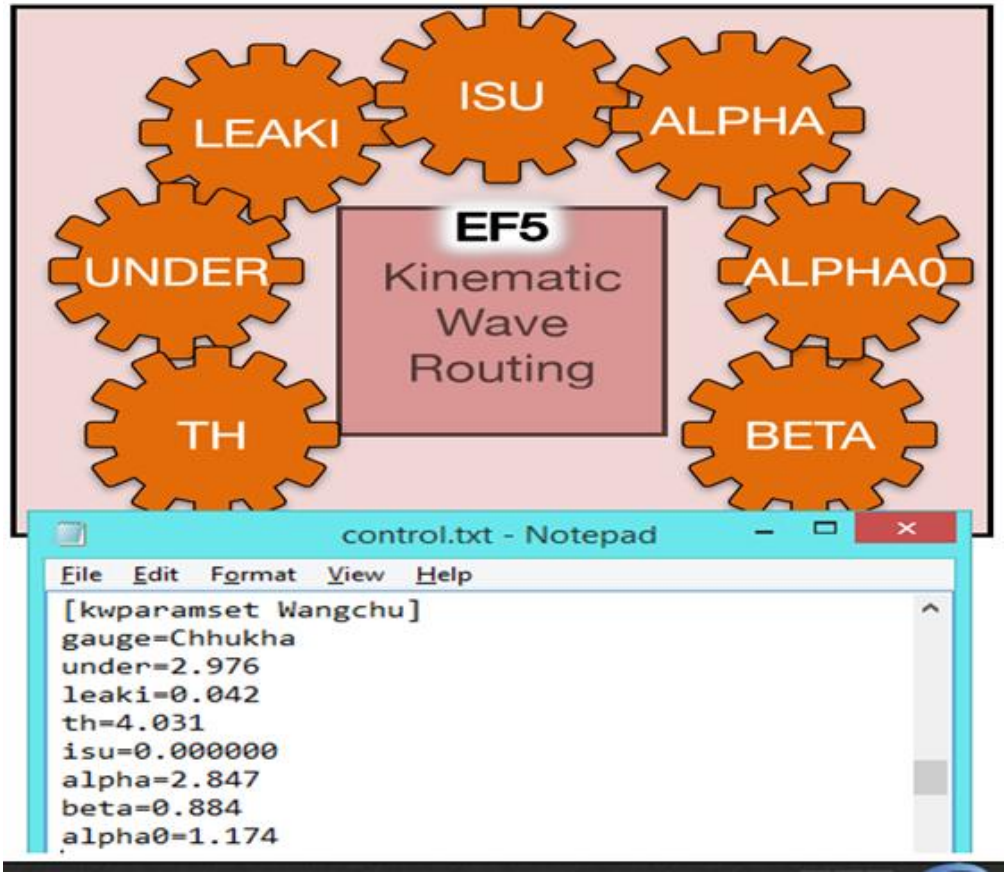

Figure 3. EF5 hydrological model kinematic wave routing parameters.

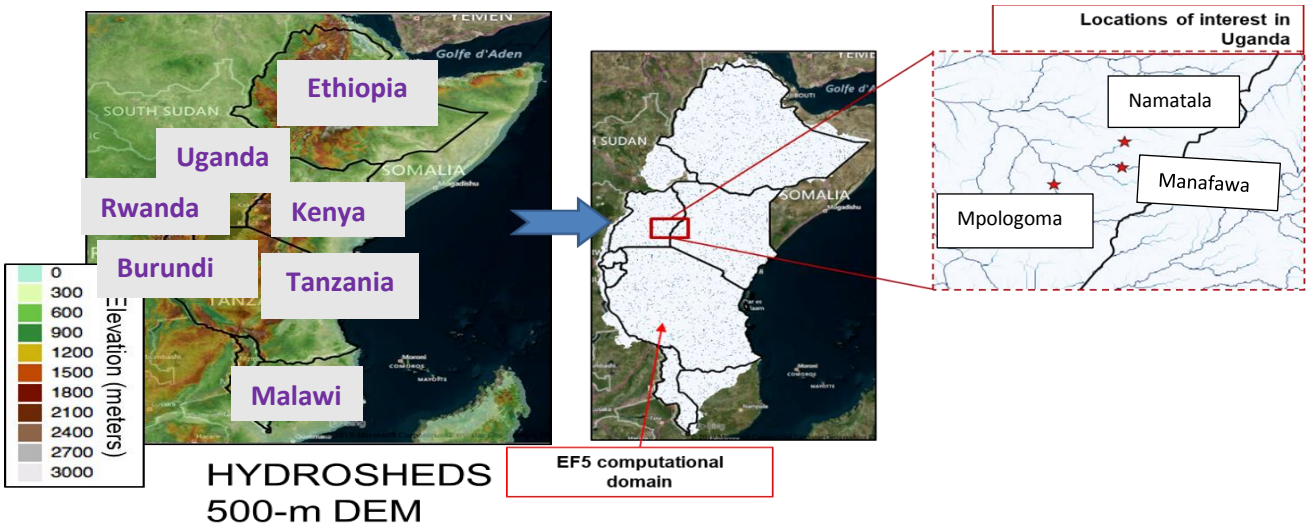

Figure 4. The regionalized hydrological model for Eastern Africa.

where calibration is impossible or gauged basins without calibrations (Gourley et al., 2016). This is achieved by using remotely sensed estimates of soil type, soil texture, and other variables to generate a priori hydrologic model parameters. Second, EF5 enables fast and accurate automatic calibration with the use of the Differential Evolution Adaptive Metropolis (DREAM) parameter optimization scheme. Third, the last major category of improvements in EF5 involve usability and user interface. This includes informative error-handling and long-term technical support and continued improvement and development by virtue of its adoption by a major U.S. government agency. We further cross-evaluate the EF5/CREST simulation with the Global Reach-Level a Priori Discharge Estimates for SWOT (Lin et al., 2019).

Forcing parameters; the earth observation satellites provide the potential to estimate precipitation on a global scale. One such unprecedented effort, the NASA Global Precipitation Measurement (GPM) mission was launched in 2014 by building upon the success of previous Tropical Rainfall Measuring Mission (TRMM) from 1997. To date, the global precipitation measurement (GPM) mission has used the Integrated Multi-satellite Retrievals for GPM (IMERG) algorithm to generate the quasi-global precipitation products at 0.1 by 0.1 arc-degree spatial resolution and 30 min temporal resolution. The GPM IMERG system runs twice in near-real-time to produce early run and late run results, where the early run has the morphing scheme only propagated forward, and the late run has the morphing scheme applied both forward and backward. Precipitation forcing to EF5/CREST in East Africa is provided by the IMERG early run products due to the near-real-time feature. Potential evapotranspiration (PET) forcing is from the USAID's FEWS NET (Famine Early Warning System Network), where PET estimates are generated using the Penman-Monteith equations. In East Africa, EF5/CREST is forced with monthly mean gridded PET estimates at 0.25 latitude by 0.25 longitude.

Cross-evaluation of longer-term simulation; any good hydrologic model relies on stream observations for calibration and validation. We are partnering with the RCMRD to deploy *in-situ* measurements in this region. However, the existing historical stream observations provided by our partners are limited in the following aspects: 1) all stream gauges are concentrated in small portions of Uganda; 2) it is unclear which daily statistics (min, max or mean) the observed values represent; 3) the observations are susceptible for underestimation as they correspond to very small unit-discharge values. Because of these limitations, we determined to pursue other sources of validation instead. Global reach-level a-Priori discharge estimates for SWOT (Lin et al. 2019) provides 35-year daily flow simulation for all rivers globally and are used for cross-evaluation. The GRADES reach has full coverage over the EF5/CREST simulation domain as shown in Figure 5. Because GRADES and EF5/CREST are developed using different DEM datasets, their stream networks do not align with each other completely. To overcome with this technical issue, we conducted two sets of cross-evaluations, that is, reach-scale and basin-scale.

For reach-scale cross-evaluation, the reaches in GRADES are paired with channel pixels in the EF5/CREST model when they share 1) similar reach length, 2) similar spatial location, 3) similar contributing drainage area. This ends up generating 124 pairs, and 10

Figure 5. GRADES Reaches overplayed on EF5/CREST Domain.

years (2001 to 2011) of their corresponding daily-mean flow values are compared. Results show that the EF5/CREST simulation based on IMERG-early satellite rainfall shows good correlation with the GRADES simulation, but higher runoff volume (Figure 6).

CREST/EF5 CAPACITY BUILDING EVENTS

In March 2018, the OU Advanced Science Team (AST) group travelled to Nairobi, Kenya and Kampala, Uganda to present the EF5 advanced training workshop and foundation EF5 training. The advanced training workshop is the follow up to the EF5 fundamental workshop. The fundamental EF5 training workshop focuses on creating a fundamental knowledge of hydrology, creating, and gathering the data needed for EF5, running and calibrating EF5, and teaching the methods to interpret the model output. The Advanced EF5 workshop training focuses on using the tools learning from the fundamental training and applying them to access advanced features in EF5. The participants were taught how to use all the ensemble outputs available. In the fundamental EF5 workshop, only the CREST water balance model was used; however, there are two other water balance models that are included in the EF5 framework. Other topics included is using distributed parameters, precipitation forcing using numerical weather predication, inundation modeling, multiple gauges, and learning Jupyter notebook to create computer generated hydrographs from the EF5 output.

The two-day advanced training on March 12-13, 2018 at RCMRD went successfully; according to the evaluations, the participants were pleased with the modules and materials of the workshop. The participants were from various occupations, including private companies, academic institutions, and government positions. Many of the participants attended the foundation EF5 training at RCMRD in March 2017 (Figure 7).

The EF5 training workshop focused on creating a fundamental knowledge of hydrology, creating, and gathering the data needed for EF5, running and calibrating EF5, and teaching the methods to interpret the model output. Specifically, the two-day EF5 workshop focused on the background and motivation of EF5, introduction to hydrologic models, EF5 overview, rainfall and PET, manual calibration, automatic calibration, interpreting and using model output, DEM practice, calibration practice, and using EF5 to monitor drought.

EF5 training focuses on a hands-on technique to teach participants how to use the EF5 modeling software. The workshop contains about eight modules that cover two full working days. The successful implementation of these

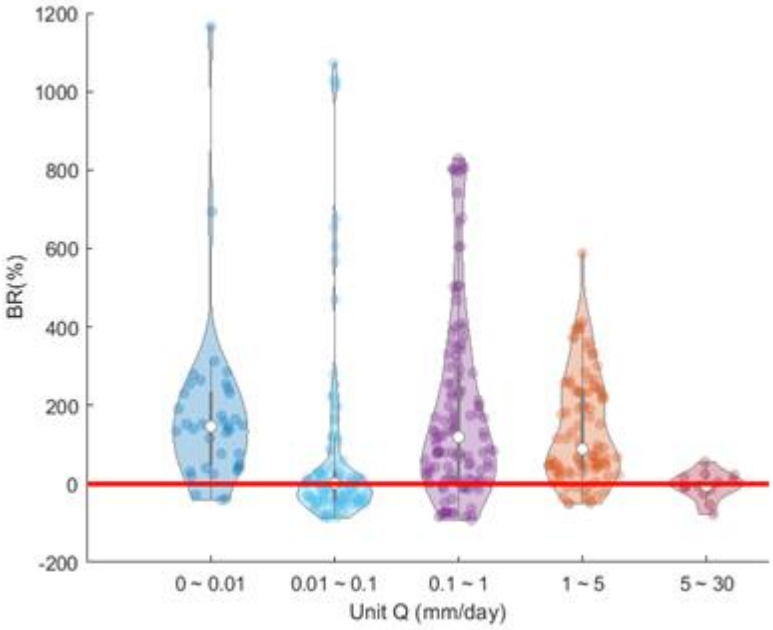

Figure 6. Relative difference of EF5/CREST and GRADES conditioned on unit flow.

Figure 7. EF5 workshop in Kampala, Uganda in March 2018.

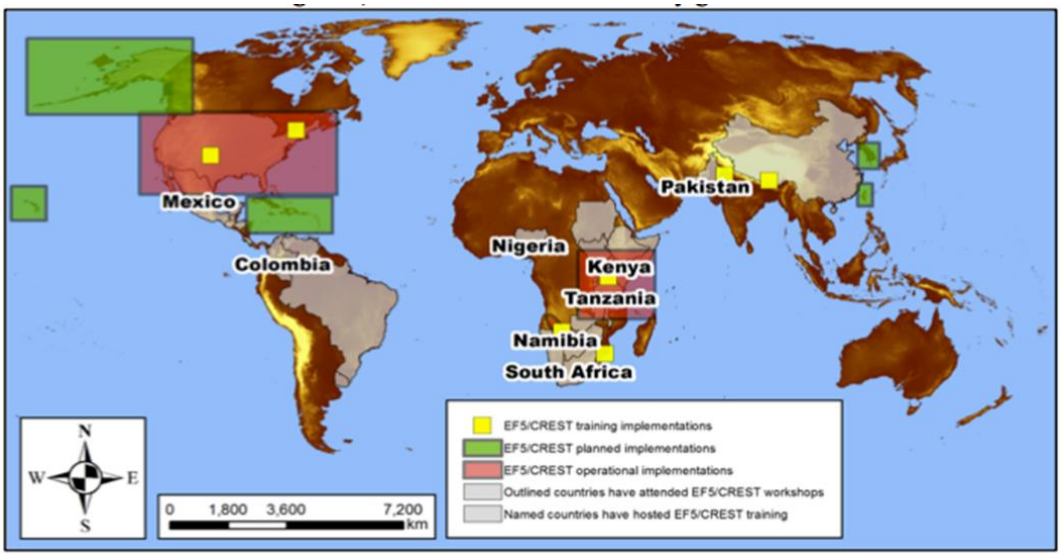

Figure 8. CREST/EF5 capacity building activities conducted across the world.

modules has been conducted over a dozen times throughout the United States, Mexico, Pakistan, Namibia, and Kenya since 2014. The advantage of this training workshop is the utilization of open source software. EF5 and QGIS, the software demonstrated in the training, are free to download and available to anyone with a computer around the world (Figure 8).

The beginning of the training focuses on the basics of hydrology to accommodate every participant; this is designed to ensure that students coming from any background can be on track. These basics include fundamental concepts of the water cycle and its inclusion in hydrologic modeling. The modules contain various training methodologies for making adult learning sessions successful, including knowledge-based and skills-based learning sessions, through means of lecturing. The combination of these two learning techniques reinforces the information needed to know about the model and demonstrations that encourage independent use.

The knowledge-based lessons make up about half of the workshop. In this method of training, the coordinator presents the facts and information needed to understand the underlying processes that the modeling software uses. This gives the workshop participants a greater understanding of the processes that are involved in the EF5 hydrologic modeling software. The other half of the training workshop utilizes skills-based learning. Workshop attendees had the opportunity to download the software and run the model on their personal laptops or computers. This supports independent practice and future use for the participants. The participants also learn how to calculate and interpret the results from the model run.

Outline of CREST/EF5 capacity building

The Ensemble Framework for Flash Flood Forecasting (EF5), is hydrological modeling software that allows users to monitor and forecast hydrological phenomena such as floods and droughts. The proposed workshop involves introductions to hydrological concepts, GIS techniques, remote sensing, and the use of hydrological model outputs. The workshop is anticipated that users will be familiar with basic hydrological and modeling concepts. Table 2 shows the EF5 workshop outline. The workshop participants will be able to install and use the EF5 model for flooding and drought forecasting on river basins of interest. The workshop participants will provide feedback on the workshop, the modeling software, desired features, and future needs that could be addressed with our system.

Advanced CREST/EF5 capacity Building

The advanced EF5 was developed to improve the fundamental EF5 hydrological modeling by including additional parameters. For example, a multiple gauge analysis was included in the advanced EF5 starting with observation locations at the upstream and calibrate it first and then calibrate the next observation location downstream. A cascaded calibration of the gauge locations is being used preparing control files under Crest param set and KW param set. In advanced EF5, output Girds to help visualize stream flow, soil moisture, return period, precipitation, and PET. The advanced EF5 also

Table 2. EF5 workshop outline.

Session 1: Welcome
Training goals; system requirements; CREST/EF5 basics; training course contents and organization; OU, HyDROS, and NASA SERVIR and Installing QGIS and TauDEM.
Session 2: Ensemble Output
Ensemble outputs with EF5; CREST model; Sacramento Soil Moisture Accounting Model; Hydrophobic model; discussion of the resolution for topographical inputs.
Review creating Digital modeling (DEM), Flow direction (FDR), Flow accumulation (FAC); review DREAM calibration; Preparation of topographical datasets for three River examples (Manafwa, Mpologoma and Namatala).
Discussion of potential pitfalls and problems.
Create hydrographs with Ensemble output for three River basin examples.
Session 3: Destributed Parameters
Review of hydrological models: distributed and lumped parameters; topographical resolution for distributed parameters; global distributed parameters; distributed parameters in EF5
Example of using distributed parameters in EF5
Review and setting up TH EF5 parameter
Session 4: Precipitation Forcing
Numerical weather prediction introduction (NWP); Global Forecast System; Weather Research and forecast Model; EF5 control file set up; EF5 (NWP) options.
Example on preparing and Executing EF5 with NWP. Download and visualize (IMERG and TRMM rainfall) and PET data for three River basins.
Session 5: Inundation Modeling
Background of inundation modeling: description of rating curves; inundation in EF5; EF5 control file set up; interpreting and using model output and Run flood inundation on three river basins
Session 7: Introduction To Jupyter Notebook
Using Jupyter notebook to create hydrograph from the simulation output
Session 6: Multiple Guages
How to use multiple gauges in a basin; set up for cascading calibration on basin in Pakistan
Use EF5 for multiple gauges and evaluate cascading calibration

included the flood inundation modeling which is an important aspect to be cautious of when floods of any kind occur. During flood inundation, if the height of water is greater than the height of the DEM, the water will overflow into the neighboring cells. Additionally, calibration is conducted on coarser resolution grid and then run on the high -resolution Shuttle Radar Topography Mission (SRTM-2) grid to save time. The advanced EF5 modeling is a multi-model ensemble expandable with new model and physics improving model results through calibration such as automatic calibration, evaluation of model skill, and defining parameters. The interpretation, analysis and use of the model result helps in flood forecasting through high-resolution immediate modeling and confidence on uncertainty.

Further, a Juypter notebook is used in the advanced EF5 for plotting the hydrograph. Therefore, the advanced EF5 developed by the OU-HyDROS has been used to provide a capacity building training in Uganda in November 2019 (Figure 9).

Capacity building/training workshops for the RCMRD hub and SERVIR network

To-date, OU Advanced Science Team (AST) has provided capacity building training to over 250 hydrologists, geographers, meteorologists, computer scientists, GIS specialists, data scientists, and many others from around 30 countries in the use of CREST/EF5 software. The OU

Figure 9. EF5 advance training.

AST team, working together with NASA and RCMRD, will continue providing both fundamental and advanced CREST/EF5 training workshops: 1)

The fundamental training workshop focuses on creating a fundamental knowledge of hydrology, creating and gathering the data, running and calibrating the models. The workshop participants will have the opportunity to download the software and run the model on their personal computers to support independent practice and future use of the software; 2) The advanced training workshop is the follow up to the fundamental ones. The Advanced EF5 workshop training focuses on using the tools learning from the fundamental training and applying them to access advanced features in the suite of CREST/EF5 system with coupled modules of landslide and inundation mapping etc.

Further, we remain committed to training partners in other countries over the long-term. The joint OU-NASA-RCMRD team will extend the capacity building training workshops to the SERVIR East and South Africa countries (Kenya, Ethiopia, Tanzania, Rwanda Tanzania, Malawi and other RCMRD member nations). We have trained the trainers, three technical staff in RCMRD so they can lead the fundamental EF5/CREST training while the OU/NASA team will focus more on advanced training. The training participants will be encouraged to complete the online training using the recently developed CREST/EF5 video (http://ef5.ou.edu/videos/) prior to the workshop to enable optimize the use of the training time and spare time to answer questions, conduct advanced tasks such as parameter optimization and model operationalization.

CALIBRATION OF EF5 MODELING IN THREE BASINS IN UGANDA (MANAFAWA, MPOLOGOMA, NAMATALA)

Hydroclimatic disaster is an emerging major threat in Uganda (CRED, 2009). Meanwhile, a rapid population growth rate is anticipated to sharply increase demands for water and create challenges for the country in achieving its development goals. Uganda has been regularly affected by water and water-related hazards. For example, flooding caused largest risks particularly in the low-lying areas and repeats almost every year. The droughts occurred in Uganda affected close to 2.4 million people between 2004 and 2013, and drought conditions in 2010 and 2011 caused an estimated $1.2 billion property loss and damage. More frequently, cascading events such as heavy rains of 2010 in the Eastern part of Uganda caused flooding which affected 33000 people including crop and infrastructure damage (OCHA, 2010) and landslides which caused 385 deaths and displacement of over 3000 people.

Through several visits and online discussion, the OU AST has worked with RCMRD, Uganda Ministry of Water and Environment, and Uganda Meteorological Authority to develop a joint plan to expand the current hydrological system coupled with new upgraded modules to Uganda. The Uganda Ministry of Water and Environment has selected the focus areas of intervention in this project; Namatala, Mpologoma and Manafwa basins (Figure 9). Figure 10 shows the early results of the CREST/EF5 hydrological modeling conducted on the three basins.

The daily gauge data, IMERG daily and TRMM 3B42RT

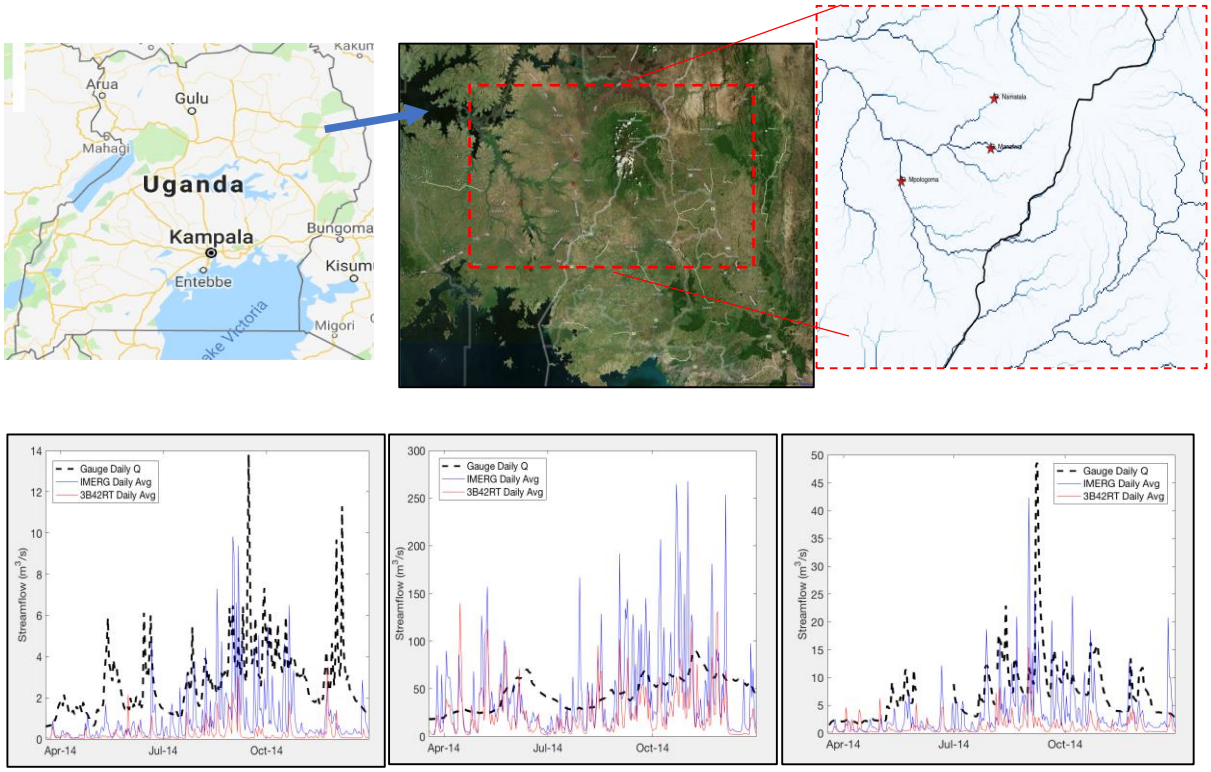

Figure 10. The EF5 hydrological modeling early results using the NASA GPM IMERG vs TRMM 3B42RT precipitation data on the three basins in Uganda.

daily precipitation data have been used to run the EF5 hydrological modeling on the three basins selected in this work. Additionally, potential evapotranspiration (PET) is a forcing parameter from the USAID's Famine Early Warning System Network (FEWS NET) where the PET is estimated using Pen-man-Monteith equations.

CONFLICT OF INTERESTS

The authors have not declared any conflict of interests.

REFERENCES

Agrawal S, Gopalakrishnan T, Gorokhovich Y, Doocy S (2013). Risk factors for injuries in landslide-and flood-affected populations in Uganda. Prehospital and Disaster Medicine 28(4):314.

Atuyambe LM, Ediau M, Orach CG, Musenero M, Bazeyo W (2011). Land slide disaster in eastern Uganda: rapid assessment of water, sanitation and hygiene situation in Bulucheke camp, Bududa district. Environmental Health 14(10):38.

Bamanya D (2007). Intra seasonal characteristics of daily rainfall over Uganda during the wet seasons. MSc thesis (unpublished), University of Nairobi, Kenya.

Boko M, Niang I, Nyong A, Vogel C, Githeko A, Medany M, Yanda P (2007). Africa climate change 2007: Impacts, adaptation and vulnerability. Contribution of working group II to the fourth assessment report of the intergovernmental panel on climate change. Cambridge University Press, Cambridge UK pp. 433-467.

Center for Epidemiology in Disasters (CRED) (2009). EM-DAT: The OFDA/CRED International Disaster Database, University Catholique de Louvain, Brussels, available at: www.emdat.be (accessed January 12, 2009).

Data Depository of the Geographic Information Systems Support Team (DDGISST) (2010). https://gist. itos.uga.edu/index.asp. Accessed May 20, 2010.

Doocy S, Russell E, Gorokhovich Y, Kirsch T (2013). Disaster preparedness and humanitarian response in flood and landslide-affected communities in Eastern Uganda. Disaster Prevention and management.

Dore M (2003). Forecasting the conditional probabilities of natural disasters in Canada as a guide for disaster preparedness. Natural Hazards 28(2):249-269.

Duclos P, Vidonne O, Beuf P, Perray P, Stoebner A (1991). Flash flood disaster-Nimes, France, 1988". European Journal of Epidemiology 7(4):365-371.

Government of Uganda (GOU) (2007). Climate Change: Uganda National Adaptation Program of Action in association with Environmental Alert, GEF and UNEP]. Kampala, Uganda.

Government of Uganda (GOU) (2009). The state of Uganda population report 2009. Addressing effects of climate change on migration patterns and women. Kampala, Uganda.

Goulden M (2008). Building resilience to climate change in lake fisheries and lake-shore populations in Uganda. Policy briefing note, Tyndall Centre for Climate Change Research, University of East Anglia, UK.

Guha-Sapir D (2010). Disasters in Numbers http://cred.be/sites/default/files/Disaster_numbers_presentation_2010.pdf. Accessed June 25, 2012.
Hulme M, Doherty R, Ngara T, New M, Lister D (2001). African Climate Change: 1900-2100. Climate Research 17(2):145-168.
Gourley J, Flamig Z, Vergara H, Kirstetter P-E, Clark III R, Argyle E, Arthur A, Martinaitis S, Terti G, Lamers J, Hong Y, Howard K (2016). The Flooded Locations and Simulated Hydrographs (FLASH) project: improving the tools for flash flood monitoring and prediction across the United States. Bulletin of the American Meteorological Society 98(2):361-372.
Intergovernmental Panel on Climate Change (IPCC) (2007). Climate Change 2007. Impacts, Adaptation and Vulnerability. Contribution of Working Group II to the Fourth Assessment Report of the Intergovernmental Panel on Climate Change, Annex I. Cambridge University Press, Cambridge, UK, 976 p.
Jonkman SN, Kelman I (2005). An analysis of the causes and circumstances of flood disaster deaths. Disasters 29(1):75-97.
Kigobe M, McIntyre N, Wheater H, Chandler R (2011). Multi-site stochastic modelling of daily rainfall in Uganda. Hydrological Sciences Journal 56(1):17-33. Accessed August 22, 2011 at http://dx.doi.org/10.1080/02626667.2010.536548,
Komutunga E, Musiitwa F (2001). Characterizing drought patterns for appropriate development and transfer of drought resistant maize cultivars in Uganda. Paper presented at the Seventh Eastern and Southern Africa Regional Maize Conference 11-15 February 2001. pp. 260-262.
Lin P, Pan M, Beck HE, Yang Y, Yamazaki D, Frasson R, Gleason CJ (2019). Global reconstruction of naturalized river flows at 2.94 million reaches. Water resources research 55(8):6499-6516.
Moe T, Pathranarakul P (2006). An integrated approach to natural disaster management: public project management and its critical success factors. Disaster Prevention and Management 15(3):396-413.
Ocowunb C (2009). Uganda: Long droughts, food shortage hit country as victims cry out for help, AllAfrica.com, accessed November 20, 2011 at http://allafrica.com/stories/200907090729.html
Osbahr H, Dorward P, Stern R, Cooper S (2011). Supporting agricultural innovations in Uganda to respond to climate risk: Linking climate change and variability with farmer perceptions. Experimental Agriculture 47(2):293-316.
Oxfam (2008). Turning up the heat: Climate change and poverty in Uganda, July 2008, Oxfam GB.
Sliuzas R, Flacke J, Jetten V (2013). Modelling urbanization and flooding in Kampala, Uganda. In Proceedings of the 14th N-AERUS/GISDECO conference pp. 12-14.
Tsarouchi G (2018). Drought and flood mitigation service for Uganda. In: EGU General Assembly 2018, 8-13 April 2018, Vienna, Austria.
UN OCHA (2010a), Eastern Uganda Landslides and Floods: Situation Report #3, OCHA, Kampala, 16 March.
World Health Organization (WHO) (2010). Landslides and floods in Bududa and Butalija districts - Health: Situation Report No. 1. www.who.int/entity/hac/y/uganda_sitrrep_5march 2010.pdf. Accessed May 9, 2010.

Vol. 15(6), pp. 243-251, June 2021
DOI: 10.5897/AJEST2021.2976
Article Number: 71E736F67065
ISSN: 1996-0786

http://www.academicjournals.org/AJEST

ACADEMIC JOURNALS
expand your knowledge

African Journal of Environmental Science and Technology

Full Length Research Paper

Occupational health impacts of climate change across different climate zones and elevations in sub-Saharan East Africa

Samuel Kruse[1*], Odilichi Ezenwanne[2], Matthias Otto[3], Tord Kjellstrom[4], Patrick Remington[5], Bruno Lemke[3], Belay Simane[6] and Jonathan A Patz[7]

[1]Department of Computer Sciences, School of Computer, Data & Information Sciences, University of Wisconsin - Madison, United States.
[2]Aaron E. Henry Community Health Services Center Inc. United States.
[3]Nelson Marlborough Institute of Technology, New Zealand.
[4]Health and Environment International Trust, New Zealand.
[5]School of Medicine and Public Health, University of Wisconsin - Madison, United States.
[6]Center for Environment and Sustainable Development College of Development Studies Addis Ababa University, Ethiopia.
[7]Global Health Institute of University of Wisconsin-Madison, United States.

Received 3 January, 2021; Accepted 25 May, 2021

Climate change will cause Sub-Saharan tropical countries to experience a disproportionate increase in the number of extremely hot days when compared to Western countries with more temperate climates. We use the High Occupational Temperature Health and Productivity Suppression (HOTHAPS) model to estimate the potential impact of rising temperatures on worker productivity in different climate regions within Ethiopia, Uganda, Rwanda, and Kenya under varying future climate change scenarios. Using population data obtained from the International Labor Organization, we also estimate productivity losses at a country-wide level. We project large inter-country and intra-country disparities in productivity losses due to varying climatic conditions and local geography. Populations living in lower elevations or in more tropical and arid zones will experience higher productivity losses than those at higher elevations with more temperate climates. We estimate that some areas could lose over 12% productivity by 2099. Comparing climate change impacts across cities, Mombasa, Kenya, is projected to suffer most, losing 13% of its labor productivity. Cities above 1500 m in elevation showed almost no productivity loss by the end of the century. Increased heat stress projected from climate change will pose added risk to workers and labor production in lower elevation settings across East Africa.

Key words: Climate change, occupational health, Sub-Saharan Africa, health impacts, heat stress, WBGT.

INTRODUCTION

The consequences of global climate change have continued to become more apparent since the early 20th century, in the backdrop of rapid industrialization, expanding economies, and continued population growth (Patz et al., 2005). Sub-Saharan tropical countries will experience a disproportionate increase in the number of

extremely hot days, when compared to Western countries with more temperate climates (Engelbrecht et al., 2015; Spector and Sheffield, 2014; Asefi-Najafabady et al., 2018). The rise in ambient temperatures will negatively impact large groups of the working population (Kjellstrom et al., 2016; Kovats and Hajat, 2008).

In this study of the East African region, we analyze the effects of Global Temperature Change (GTC) on workers in the countries of Rwanda, Ethiopia, Kenya, and Uganda. While global temperature averages are rising, climate change impacts for a given locale are highly dependent on its geography and climate classification. To better understand regional variation of potential productivity losses due to climate change, we also study select cities with varying geographic and climate conditions (Table 2).

Workers in these countries who carry out various forms of manual labor outdoors (in sun or shade) or work indoors without air conditioning are the most vulnerable and may be forced to considerably reduce their work time because of the heat (Kjellstrom et al., 2016; Nilsson and Kjellstrom, 2010). Loss in hourly productivity with increasing ambient temperature occurs as humans initially try to adapt by physiological (sweating) and behavioral (self-pacing) mechanisms in an effort to maintain thermoregulation; should these mechanisms fail, a spectrum of heat-related illnesses can occur if interventions are not taken to reduce the core body temperature (Cheung et al., 2016).

Reduced work capacity and labor productivity losses begin to occur when Wet Bulb Global Temperature (WBGT) exceeds 26°C, rising steadily until about 40°C when labor becomes almost impossible to sustain (Kjellstrom et al., 2009; Sahu et al., 2013). The High Occupational Temperature Health and Productivity Suppression (HOTHAPS) programme models the relationship between WBGT and work productivity. We ran HOTHAPS on regional climate data collected from Potsdam Institute's Intersectoral Impact Model Intercomparison Project (ISI-MIP) to model how worker productivity in Eastern Africa may be affected by climate change.

While understanding how WBGT varies with geography is vital to understanding regional work loss, geographic variables are not explicit parameters in the model but are implicitly present in the WBGT. Elevation strongly affects temperatures (and thus WBGT), with mean decreases in temperature of 6.5°C for every 1000 m ascended (Lapse Rate, 2016; Fairbridge and Oliver, 1987). We therefore compared across countries within East Africa with markedly different elevations to assess risks from climate change on worker heat stress and potential losses in labor productivity.

MATERIALS AND METHODS

The model we use, HOTHAPS, derives estimates for the heat load on workers under different climatic conditions. The model uses Wet Bulb Globe Temperature (WBGT) to directly estimate climate effects on the loss of work productivity at different ambient temperature levels for workers at different levels of labor intensity, Kjellstrom et al. (2018) discuss more on the treatment of the methodology. The WBGT is derived from daily recorded climate data, combining air temperature, humidity, wind speed, and solar radiation. Direct sun exposure increases WBGT so all work is assumed to be done in the shade or indoors without air conditioning for this study. Thus, WBGT has been employed as a more comprehensive and conservative indicator of the risk of heat exposures in workplace settings (Parsons, 2014).

Model and parameters

We used data sets of WBGT from the Potsdam Institute's Intersectoral Impact Model Intercomparison Project (ISI-MIP), from the four main Representative Concentration Pathway (RCP) scenarios of the Intergovernmental Panel on Climate Change (IPCC): RCP2.6, RCP4.5, RCP6.0, and RCP8.5. These scenarios describe a range of radiative forcing levels by the year 2100 given certain socio-economic, technological, and climate policy assumptions (Table 1).

The highest of these values (RCP8.5) corresponds to a "business as usual" where emissions levels continue to rise without preventive actions allowing radiative forcing to reach 8.5 W/m^2 by the end of the century. Whereas the 2.6 W/m^2 scenario represents a "best case" scenario where Global Temperature Change (GTC) stops at +1.6°C. RCP6.0 represents an intermediate scenario with stabilization of emissions and a projected increase in the GTC of about 2.7°C by the end of the century with radiative forcing reach as high as 6.0 W/m^2 (van Vuuren et al., 2011). For this study, we analyze both the RCP6.0 and RCP2.6 scenarios. These RCP values act as parameters for all the models included in the ISI-MIP climate models: HadGEM2, NORES, GFDL, IPSL, and MIROC. We use HadGEM2 and GFDL based on previous findings that showed HadGEM2 to produce results close to the upper limit of models and GFDL to produce results close to the lower limit of IPCC projections (Collins et al., 2013). Additionally, the mid-point estimates of these two models were close to averages of all IPCC models (Collins et al., 2013; Kjellstrom et al., 2018).

These models use climate data that were obtained from Health and Environment International Trust (HEIT) through their website www.climatechip.org, an online database that comprises historical climate data and future estimates for different climate scenarios. ClimateCHIP provides monthly averages of the daily recorded Maximum and Mean WBGT for all locations across the world. We derive another WBGT variable to represent the midpoint between the Maximum and Mean WBGT values: Mid WBGT.

These variables allow us to use the "4 + 4 + 4" method to approximate a worker's total hours of WBGT exposure for a month. This method assumes 12 h of daylight each day, each variable is normally distributed, and each variable corresponds to a set of time slices (totaling four hours of the day). The Maximum variable corresponds to the hottest time of day (10 am – 2 pm). The Mean variable is the midpoint between the daily Maximum WBGT score and the daily minimum score (coldest at night). For this reason, we divide the Mean variable times slice into the two-hour timeslots at

*Corresponding author. E-mail: sdkruse@wisc.edu.

Table 1. Main characteristics behind selected RCP scenarios.

Scenario component	RCP2.6	RCP4.5	RCP6	RCP8.5
Greenhouse gas emissions	Very low	Medium-low mitigation; Very low baseline	Medium baseline; high mitigation	High baseline
Agricultural Area	Medium for cropland and pasture	Very low for both cropland and pasture	Medium for cropland but very low for pasture (total low)	Medium for both cropland and pasture
Air Pollution	Medium-Low	Medium	Medium	Medium-high
Included in Results	Yes	No	Yes	No

the beginning and end of each day (6 am – 8 am, 4 pm – 6 pm). The Mid variable then accounts for the time slots 8 am – 10 am and 2 pm – 4pm. We assume a normal distribution for each of these variables with a standard deviation of 2°C. The area under the curve for each variable represents total amount of time spent near that WBGT score. We partition each distribution into 1°C bins (25-25.99°C) and then use the area under the curve to approximate the amount of time each day is spent at that temperature. We then sum the number of hours in each bin across all distributions which approximates the total hours of exposure.

In addition to WBGT, the intensity of physical exertion during exposure period-generating internal body heat-contributes to the risk of heat stress. We consider three intensity classes: 200, 300, and 400 Watts (W) of metabolic rate. Each one of these levels correspond to increasing levels of exertion from light clerical work at 200 W to construction labor or agricultural work at 400 W. We use the sums of hours and the intensity of the labor activity to calculate productivity the work loss at each intensity using exposure response curves of the general form (cumulative Gaussian distribution):

$$\text{Productivity loss } \mathbf{(y)} = 0.5[1 + \text{erf}(x-\mu/\sigma\sqrt{2})]$$

where μ and σ are the mean and standard deviation of the associated normal curve. The output is a percent of work lost for the duration of exposure. We aggregate that percent loss for each hour spent in that bin and summarize our results by aggregating decadal averages of productivity loss through the end of the century (2099).

Selected population and employment data

When calculating productivity losses for a country, we use gridded population projections to weight how much productivity loss can be attributed to a given grid cell. Just as in the International Labour Organization report, "Working on a warming planet" (ILO, 2019), we combined population data from Columbia University's Gridded Population of the World and employment-to-population ratios ILOSTAT database to generate estimates for employment numbers for specific economic sectors in each country: agriculture, construction, industry and services. Based on the country-specific proportion of these economic sectors, and assumed metabolic rates for each industry, we estimate productivity losses in each country up until 2099 (Kjellstrom et al., 2018). Our estimates show the effects on individual workers depending on work intensity in Watts.

Selection of cities

For each country we selected two cities to investigate. We picked the capital of each country and a city with distinct geographical characteristics (climate classification or elevation) to explore intra-country work loss variation (Table 2).

RESULTS AND DISCUSSION

For all our results, we use the midpoint between GFDL and HadGEM2 projections. Under both emission scenarios, RCP2.6 and RCP6.0, work losses varied by region. There were greater work losses in RCP6.0 than in RCP2.6 scenario for each country. In general, cities at higher elevations experienced fewer work losses.

Selected countries

All our projections for productivity losses of low-intensity work (200W) were less than 1% for every country throughout the end of the century. Our projections for moderate work intensity (300W) showed no losses in Rwanda and less than 1% loss in Ethiopia but Kenya and Uganda may experience up to 1.4 and 2% work loss, respectively, by year 2095. Figure 1 show productivity losses for different intensity work by Country for (2091-2099) for RCP6.0 using midpoint between GFDL and HadGEM2 using population data from Columbia University's Gridded Population of the World and employment-to-population ratios ILOSTAT database

According to the Central Intelligence Agency World Fact Book, Rwanda and Ethiopia have the 11th and the 16th highest mean elevation out of all the countries in the world, respectively. These high mean elevations may mean fewer days of extreme heat and thus fewer losses in productivity. Even for high-intensity work, we project Rwanda will lose <1% of work productivity through the year 2095. While large swathes of Ethiopia are semi-arid or desert climate zones, much of the country is at high elevation, and we find only ~1.3% productivity loss by the end of the century for high-intensity work (Figure 1). Kenya and Uganda will experience greater losses under the same scenarios. According to our model, Uganda will experience the greatest total work loss out of the

Table 2. Geographic information for selected cities; population data are 2015 grid cell population estimates from Columbia University's Gridded Population of the World; note that Mombasa and Addis Ababa are contained by multiple grid cells, so we combine them here

City	Latitude and Longitude	Elevation	Climate Classification	Grid cell Population
Kigali, RWA	-1.75, 30.25	1,567 m	Tropical Savannah (Aw)	1,755,790
Gisovu, RWA	-2.25, 29.25	2,200 m	Tropical Savannah (Aw)	1,116,510
Addis Ababa, ETH	9.25, 38.75 & 8.75, 38.75	2,344 m	Humid Subtropical climate (Cwb)	4,576,243
Dire Dawa, ETH	9.75, 41.75	1,275 m	Warm semi-arid climate (Csa)	245,425
Nairobi, KEN	-1.25, 36.75	1,794 m	Humid subtropical highland (Cwb)	5,617,037
Mombasa, KEN	-3.75, 39.75 & -4.25, 39.75	50 m	Tropical Savanna (As)	1,975,810
Kampala, UGA	0.25, 32.75	1,200 m	Tropical Monsoon (Am) Equatorial Climate (Af)	3,597,145
Gulu, UGA	2.75, 32.25	1,100 m	Tropical Savannah (Aw)	358,891

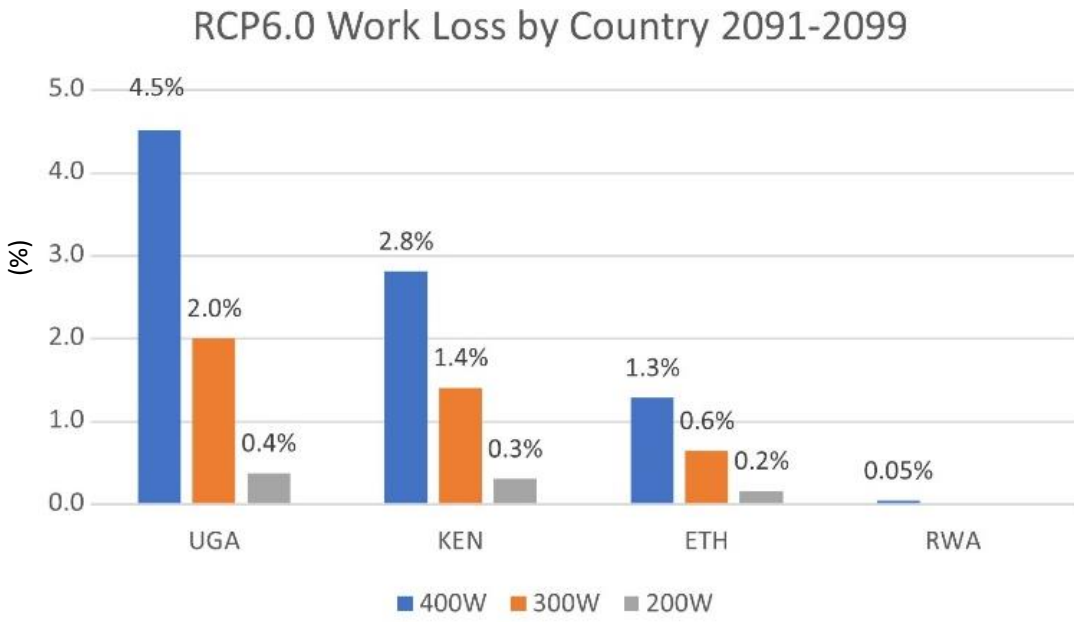

Figure 1. Productivity Losses for different intensity work by Country.

countries studied losing as much as 4.5% productivity by 2099 at 400W intensity (metabolic rate) whereas Kenya will lose 2.8% productivity.

Selected cities

Using the midpoint between HadGEM2 and GFDL as well, we provide some highlights of the city-level data. Work loss levels varied from city to city, even between cities in the same country. For example, even at 400W intensity, Nairobi, Kenya may not experience any loss in productivity by the end of the century, whereas Mombasa, Kenya is projected to lose 13% productivity. Like Nairobi, the cities Gisovu, Kigali, and Addis Ababa are located above 1500 meters in elevation and showed almost no productivity loss by the end of the century under our model. All other locations showed rising trends in productivity losses from the 2005 to 2099 (Figure 2). Since both Addis Ababa and Mombasa span two grid cells, results for these cities are presented as the midpoint between the grid cells for convenience. Work loss over next century under RCP6.0 for high intensity work; Nairobi, Kigali, Gisovu, and Addis Ababa had 0% work loss over the period, the latter three of which were excluded from Figure 2.

We project fewer work losses under the RCP2.6 scenario (Figure 3) for each city than in the RCP6.0

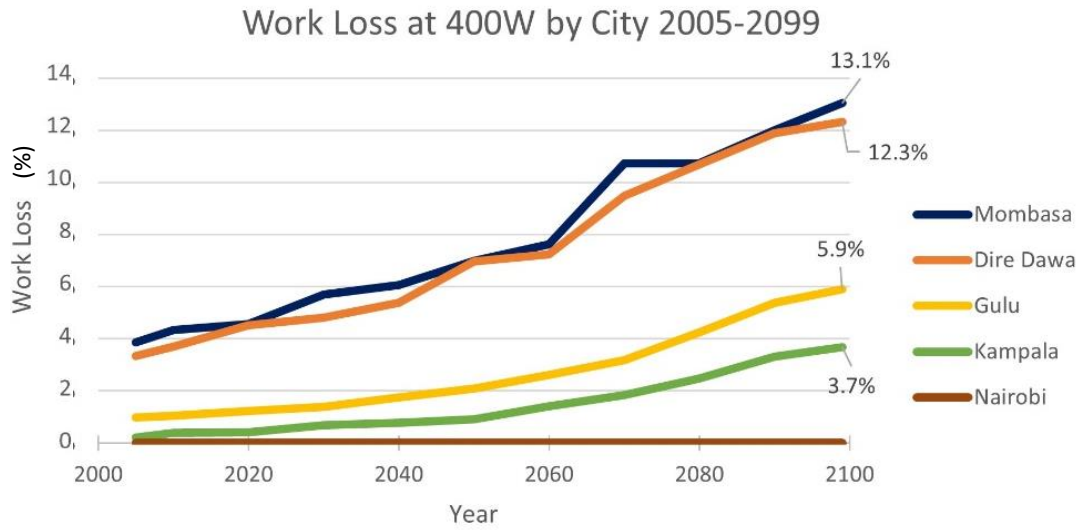

Figure 2. Work Loss over next century under RCP6.0.

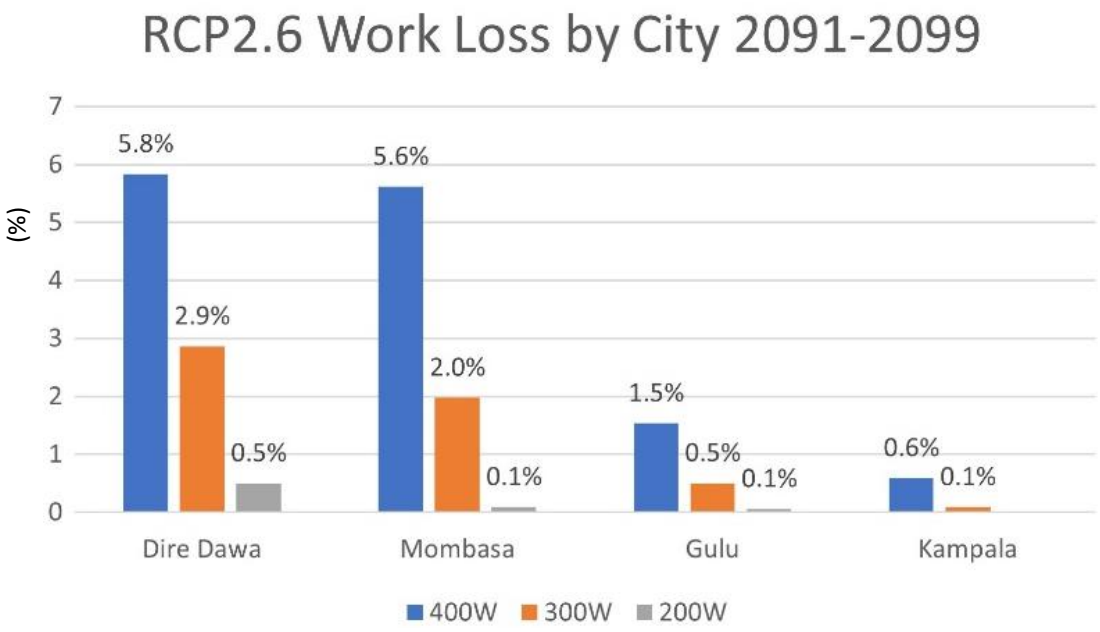

Figure 3. Work loss for all cities under RCP2.6.

scenario (Figure 4). Even so, both Mombasa and Dire Dawa still may lose more than 5% of work productivity by the end of the century under RCP2.6 scenario. We project that Mombasa will experience the greatest productivity losses out of the selected cities; its elevation is just 50 meters above sea level. For high intensity labor, we see as much as 13% work loss by the end of the century. In Dire Dawa, we project 12.3% productivity loss by the end of the century. For the same period, Gulu can expect as much as ~6% and Kampala, ~3.7%. Work loss for all cities under RCP2.6 at all intensities; Nairobi, Kigali, Gisovu, and Addis Ababa had 0% work loss over the period, the latter three of which were excluded from Figure 3. Work loss for all cities under RCP6.0 at all intensities; Nairobi, Kigali, Gisovu, and Addis Ababa had 0% work loss over the period, the latter three of which were excluded from Figure 4.

Our findings for worker productivity in East Africa are consistent with prior climate change studies in other global regions. Our results further show work loss variance across areas with markedly diverse geography, particularly varying by elevation and climate zone

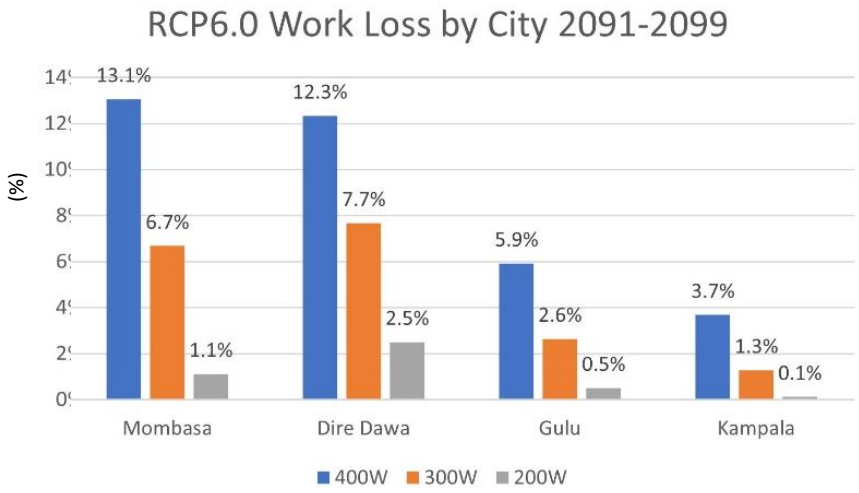

Figure 4. Work loss for all cities under RCP6.0 at all intensities; Nairobi, Kigali, Gisovu, and Addis Ababa.

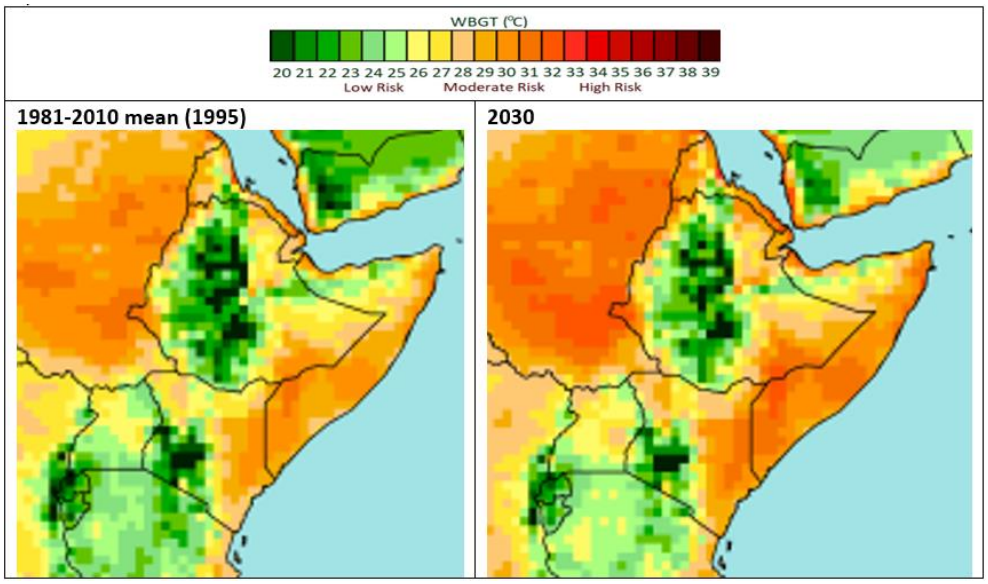

Figure 5. Monthly mean of daily maximum WBGT in East Africa at two times, 1995 and 2030; the colors represent risk of heat exhaustion and productivity loss.

classification. In every country except Rwanda, we see large intra-country variation in projected work loss (Figure 5). The frequency and intensity of these extreme heat stress days are projected to increase with climate change. While this may result in a reduction in worker productivity, it also may lead to higher rates of morbidity and mortality with the rate of increase varying by region (Hoegh-Guldberg et al., 2018). Even with highly variable local effects, rising global mean surface temperatures (GST) has been noted to be the most predictable impact of anthropogenic emission-induced climate change (Collins et al., 2013). Areas at high elevation like Addis Ababa and Kigali enjoy temperate climates with relatively low mean monthly temperatures even during the hotter parts of the year. Subsequently, losses in work productivity in these high elevation areas, even for the heavy intensity work groups under a more extreme emission scenario (RCP6.0), showed a minimal decrease in productivity (Figures 6 and 7).

Of the four countries studied, three of their capitals (which are their largest cities by population) are elevated 1,500 m above sea level (Figure 7). These cities experienced almost no work loss under any scenario. Figure 7 suggests a relationship between work loss and

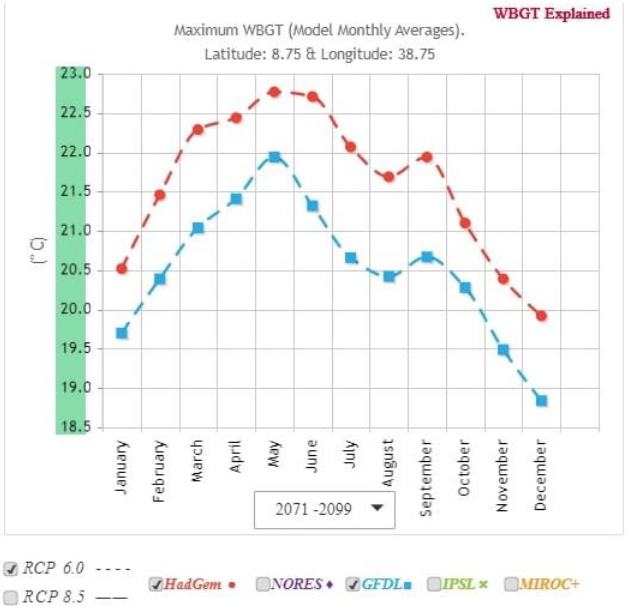

Figure 6. Monthly Distribution of Maximum WBGT for Addis Ababa (2071-2099, RCP6.0); Image from https://climatechip.org/your-area-tomorrow.

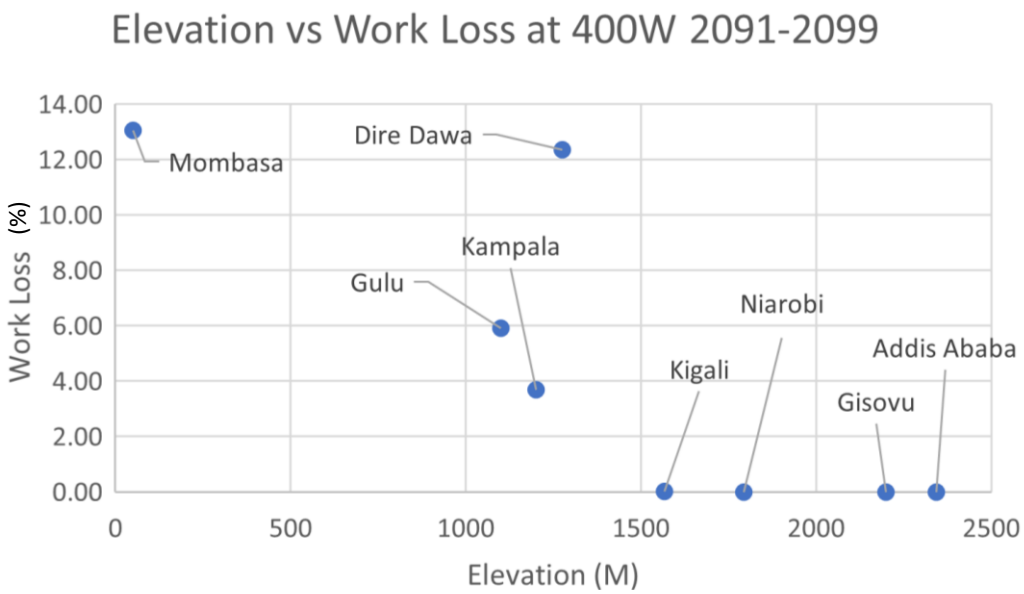

Figure 7. Elevation vs Work Loss at 400W for 2091-2099.

elevation but further research with more locations and data is needed to better understand a possible relationship. Any further research examining the relationship between elevation and work loss in this region should consider climate classification as another variable of interest. For example, Dire Dawa has a higher elevation than Kampala but we project almost 3 times more work loss in Dire Dawa. Its relatively high mean monthly temperatures (Figure 8) and its comparatively high work loss for its elevation may be explained its warm semi-arid (Csa) climate classification.

Limitations

One limitation of our country-wide work loss projections is

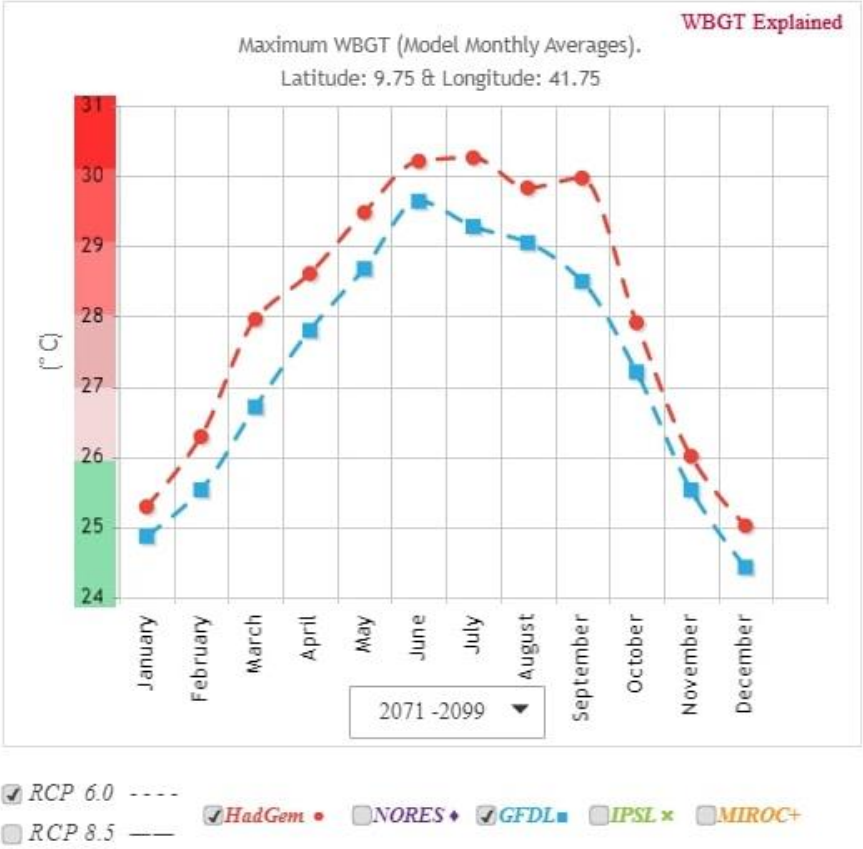

Figure 8. Monthly Maximum WBGT Averages for Dire Dawa (2071-2099, RCP6.0); Image from https://climatechip.org/your-area-tomorrow.

the reliance on population data in each grid cell to weight each grid cell's contribution to overall productivity loss. As certain effects of climate change intensify, migratory patterns may shift in unexpected ways. Extreme weather events (drought, storms, floods, and etc.) will occur with greater frequency with GTC (Cattaneo et al., 2019). Assessment of adaptive strategies, such as scheduled time away from work during peak temperature months, switching work to night-shifts, or other typical extreme heat interventions would involve a full suite of adaptation scenarios (and associated uncertainties) that are beyond the scope of this manuscript addressing altered risk levels from climate change in the region.

Conclusion

Climate change is expected to increase WBGT in Eastern Sub-Saharan Africa which will, in turn, decrease labor productivity in parts of the region. Some large cities like Mombasa may experience significant labor productivity losses under RCP6.0 scenario. The impact of climate change on workers in these countries varies significantly across different climate zones and elevations. Further research is needed to establish a quantitative relationship between climate classification, elevation, and productivity loss. Although populations in areas of high elevation appear to be relatively spared from productivity loss, a significant proportion of the population in other regions will be directly affected by climate change. To mitigate productivity losses induced by spikes in WBGT, we must keep average global temperatures from surpassing +1.6°C. This will require significant and immediate reductions in global greenhouse gas emissions.

CONFLICT OF INTERESTS

The authors have not declared any conflict of interests.

ACKNOWLEDGMENTS

Funding support for this research came from NIH Fogarty, grant #0123456789, "Global Environmental and Occupational Health (GEOHealth) Hub for East Africa."

REFERENCES

Asefi-Najafabady S, Vandecar KL, Seimon A, Lawrence P, Lawrence D (2018). Climate change, population, and poverty: vulnerability and exposure to heat stress in countries bordering the Great Lakes of Africa. Climatic Change 148(4):561-573.

Cheung SS, Lee JKW, Oksa J (2016). Thermal stress, human performance, and physical employment standards. Applied Physiology, Nutrition, and Metabolism 41(6):148-164.

Collins M, Knutti R, Arblaster J, Dufresne JL, Fichefet T, Friedlingstein P, Gao X, Gutowski WJ, Johns T, Krinner G, Shongwe M (2013). Long-term Climate Change: Projections, Commitments and Irreversibility. In: Climate Change 2013: The Physical Science Basis. Working Group I to the Fifth Assessment Report of the Intergovernmental Panel on Climate Change. Cambridge University Press pp. 1029-1136.

Cattaneo C, Beine M, Fröhlich CJ, Kniveton D, Martinez-Zarzoso I, Mastrorillo M, Millock K, Piguet E, Schraven B (2019). Human Migration in the Era of Climate Change. Review of Environmental Economics and Policy 13(2):189-206.

Engelbrecht F, Adegoke J, Bopape MJ, Naidoo M, Garland R, Thatcher M, Gatebe C (2015). Projections of rapidly rising surface temperatures over Africa under low mitigation. Environmental Research Letters 10(8):085004.

Fairbridge RW, Oliver JE (1987). Lapse rate. In: Climatology. Encyclopedia of Earth Science. Springer, Boston, MA. https://doi-org.ezproxy.library.wisc.edu/10.1007/0-387-30749-4_105

Hoegh-Guldberg O, Jacob DM, Taylor M, Bindi S, Brown I, Camilloni A, Diedhiou R, Djalante KL, Ebi F, Engelbrecht J, Guiot Y, Hijioka S, Mehrotra A, Payne SI, Seneviratne A, Thomas R, Warren G, Zhou (2018). Impacts of 1.5ºC Global Warming on Natural and Human Systems. In*:* Global Warming of 1.5°C. An IPCC Special Report on the impacts of global warming of 1.5°C above pre-industrial levels and related global greenhouse gas emission pathways, in the context of strengthening the global response to the threat of climate change, sustainable development, and efforts to eradicate poverty *[Masson*-Delmotte, V., P. Zhai, H.-O. Pörtner, D. Roberts, J. Skea, P.R. Shukla, A. Pirani, W. Moufouma-Okia, C. Péan, R. Pidcock, S. Connors, J.B.R. Matthews, Y. Chen, X. Zhou, M.I. Gomis, E. Lonnoy, T. Maycock, M. Tignor, and T. Waterfield (eds.)]. In Press.

Kjellstrom T, Briggs D, Freyberg C, Lemke B, Otto M, Hyatt O (2016). Heat, Human Performance, and Occupational Health: A Key Issue for the Assessment of Global Climate Change Impacts. Annual Review of Public Health 37:97-112.

Kjellstrom T, Freyberg C, Lemke B, Otto M, Briggs D (2018). Estimating population heat exposure and impacts on working people in conjunction with climate change. International Journal of Biometeorology 62(3):291-306

Kjellstrom T, Gabrysch S, Lemke B, Dear K (2009). The 'Hothaps' programme for assessing climate change impacts on occupational health and productivity: an invitation to carry out field studies. Global Health Action 2(1):2082.

Kovats RS, Hajat S (2008). Heat Stress and Public Health: A Critical Review. Annual Review of Public Health 29(1):41-55.

Lapse rate (2016). In Encyclopaedia Britannica. Encyclopædia Britannica. https://www.britannica.com/science/lapse-rate

Nilsson M, Kjellstrom T (2010). Climate change impacts on working people: How to develop prevention policies. Global Health Action 3(1):5774. doi:10.3402/gha.v3i0.5774

Parsons K (2014). Human Thermal Environments. Boca Raton: CRC Press.

Patz JA, Campbell-Lendrum D, Holloway T, Foley JA (2005). Impact of regional climate change on human health. Nature 438(7066):310-317.

Peel MC, Finlayson BL, McMahon TA (2007). Updated world map of the Köppen-Geiger climate classification. Hydrology and Earth System Sciences 11(5):1633-1644.

Sahu S, Sett M, Kjellstrom T (2013). Heat exposure, cardiovascular stress and work productivity in rice harvesters in India: implications for a climate change future. Industrial Health 51(4):424-431.

Spector JT, Sheffield PE (2014). Re-evaluating Occupational Heat Stress in a Changing Climate. *The Annals of Occupational Hygiene 58*(8):936-942.

van Vuuren DP, Edmonds J, Kainuma M, Riahi K, Thomson A, Hibbard K, Rose SK (2011). The representative concentration pathways: An overview. Climatic Change 109(1-2):5-31. doi:10.1007/s10584-011-0148-z

Vol. 15(6), pp. 252-261, June 2021
DOI: 10.5897/AJEST2020.2960
Article Number: 2D78B4167107
ISSN: 1996-0786

http://www.academicjournals.org/AJEST

ACADEMIC JOURNALS
expand your knowledge

African Journal of Environmental Science and Technology

Full Length Research Paper

Optimization of oxygen consumption and reduction of organic matter from waste during the fermentation phase: Case of the composting platform in Lomé, Togo

Edem Komi Koledzi[1*], Kwamivi Nyonuwosro Segbeaya[1,2], and Nitale M'Balikine Krou[2]

[1]Laboratory of Waste Management, Treatment and Recovery (GTVD), Faculty of Sciences, University of Lomé, P. O. Box 1515 Lomé-Togo.
[2]Laboratory of Sanitation, Water Science and Environment (LASEE), Faculty of Science and Technology, University of Kara, P. O. Box 404 Kara, Togo.

Received 2 December, 2020; Accepted 9 June, 2021

In the context of carbon financing it is required that the rate oxygen inside the windrows exceeds 8% to avoid anaerobic decomposition. Thus, the objective of this study is to optimize oxygen consumption and reduce organic matter in the waste during the fermentation phase. Windrow turning is monitored, which includes monitoring of temperature, pH, organic matter, humidity and certain metals.Temperature monitoring showed a gradual decrease until stabilization at room temperature, indicating the maturity of the compost. With a slight increase in all swaths, the pH remained alkaline. The humidity in the windrows promoted good aerobic degradation of the composted waste. The organic matter in these windrows has decreased to values that agree with standards. The present study has demonstrated the importance and influence of the oxygen content and the production of carbon dioxide on the mineralization of organic matter, especially during the fermentation phase.

Key words: Flipping, compost, oxygen and carbon dioxide levels.

INTRODUCTION

Composting is an ancestral technique, one of the most widely used ways of recovering materials from household wastes. It limits the use of landfill or incineration. Among the organic matter transformation processes, composting is particularly interesting for the transformation of organic matter, because it makes it possible to considerably reduce the mass and volume of the initial effluents, thus allowing a reduction in transport costs. It is a controlled process of degrading organic materials of plant or animal origin. During intense transformations of organic matter (OM), a transfer of pollution to the atmosphere is possible depending on the substrates put to compost and the methods of composting (Tchegueni et al., 2012). Faced with this observation, ensuring the environmental impact of composting, in particular for organic matter in household waste is essential. However, during this process a significant amount of water and dry matter is lost (about 50% of the initial masses), mainly in gaseous

*Corresponding author. E-mail: edemledzi@yahoo.fr. Tel: 00228 90198535.

form. This aerobic biological treatment allows a return to the soil of stabilized organic matter. In this process, the degradation of the substrates is marked by the decrease in organic matter, also indicating that the compost obtained is mineralized (Tchegueni et al., 2012). When aeration is done well, we obtain a mature compost after three months. In fact, the degree of maturity of a compost is the stage at which the compost no longer has a negative effect on plants (Koledzi, 2011). Composting also helps to reduce the emission of methane, which is a Greenhouse Gas (GHG) responsible for global warming (Sánchez et al., 2015). To reduce the risk of methane emissions, this aerobic process requires large amounts of oxygen, especially at the initial stage. Aeration is the source of oxygen, and thus is found to be an essential factor for aerobic composting. When the oxygen supply is not sufficient, the growth of aerobic microorganisms is limited, which slows down decomposition (Bokobana et al., 2017). Thus, good aeration is essential for efficient composting. This can be achieved if the physical quality of the materials (particle size and water content), the size of the pile and the ventilation are controlled and if the waste mixture is frequently turned. The fermentation phase requires controlling humidity, temperature and air supply. Oxygen is supplied in various ways. The turning of the swath, the air blowing (mechanical ventilation system using fans or aeration pipes inside the windrow) and the natural circulation of air between the particles of material first are methods commonly used to ensure the supply of air. In fact, aeration provides the oxygen necessary for good biological degradation of the substrates (Turan and Ergun, 2008). According to the same study, oxygen consumption is generally high during the fermentation phase and decreases as the composting process progresses. Some authors have shown that the presence of oxygen at a minimum threshold of around 5 % oxygen is essential for the successful completion of composting (Puyuelo et al., 2010). This oxygen is also consumed by microorganisms during their activity and on the other hand by oxidation reactions. For others still, the oxygen level is directly related to the percentage of gaps (porosity) in the material to be composted, to the particle size of the particles present and to the humidity of the compost (Mustin, 1987). This is because the higher the porosity, the easier the air circulation. Humidity acts in the opposite direction. Decomposition of organic matter is inhibited when the water content drops below 20 %. If it exceeds 70 %, the water begins to fill the waste spaces and prevents oxygen exchange, thus causing conditions favorable to anaerobiosis (Toundou, 2018). Optimal composting is obtained for values of 30 to 36% porosity in the mass (Mustin, 1987). In addition, if the grain size is too fine, it causes "suffocation" of the windrow, if it is too coarse it can be synonymous with drying out due to the significant air circulation; grinding of the waste is therefore necessary to obtain a favorable particle size and a good mixture of the substrates. According to the same study, the oxygen level changes over time: aerobic microorganisms use oxygen and release CO_2, which tends to deplete the environment in O_2, but the air circulation in the heap of compost renews the atmosphere and enriches the environment with O_2. An intervention (turning over) may then be necessary to restore the aerobic conditions of the composting. Several indicators are used to characterize the aerobic evolution of the composting process. However, monitoring the level of oxygen (O_2) seems to be a scientifically more reliable indicator than monitoring the level of CO_2 to characterize the aerobic evolution of a compost heap. Insofar as a minimum level of oxygen is necessary for good aerobic degradation and that composting platforms must limit emissions of carbon dioxide, which is a GHG, it is urgent to find alternatives to optimize oxygen consumption and the production of carbon dioxide.

In Togo, the composting platform of the company ENPRO has been involved in the carbon credit process for more than six years, in 2013. In fact, in the context of carbon financing where the platform is involved, the oxygen level inside the windrows must exceed 8% to avoid anaerobic decomposition, a value taken above that indicated in the literature to guarantee optimal aeration. Thus, the objective of this study is to optimize the oxygen consumption and the production of carbon dioxide in windrows. To do this, windrow turning is monitored, which includes monitoring of the evolution of oxygen (O_2), carbon dioxide (CO_2), organic matter (OM), humidity and certain metals.

MATERIALS AND METHODS

Material

The raw materials used in this study are the biodegradable fractions of urban waste obtained after sorting unwanted materials on the site of the NGO “ENPRO” Clean Natural Ecosystem in Lomé. Figure 1 shows the waste collected and dumped on the composting site.

Five compost heaps (windrows) were made after sorting the waste from various pre-collection structures in the city of Lomé; these are windrows A, B, C, D, and E.

Methods

Composting methods

In this study, composting in heaps or windrow is adopted. In fact, the waste dumped on the site is sorted and free of non-biodegradable materials on a sorting table (Figure 2). In Lomé, the rate of sand in the waste is between 35-44 % (Koledzi, 2011)[2]. Thus, a mesh of 10 mm on the table reduces the proportion of sand.

To have the piles or windrows on the site, the putrescible or compostable waste obtained after sorting is layered (Figure 3) and gradually watered with a quantity of water proportional to the humidity of this waste. To speed up the composting process, a few kilograms of already decaying waste from an old pile launched some time ago are incorporated into the new waste during the pile-up. According to a specific method, the piles are turned to facilitate

Figure 1. Waste collected and dumped on the composting site.

Figure 2. Sorting tables.

Figure 3. Windrows in preparation.

the supply of oxygen in order to avoid anaerobic transformation which can lead to the formation of foul-smelling gases and carbon dioxide (Figure 3). Windrows A and B are turned weekly. For C and D, we thought that by bringing the reversals together during the first two weeks when the activity is intense, we could therefore keep the oxygen level above 8 %. The following formula was used where we do four turnovers in the first two weeks: 3rd day, 5th day, 10th day, 15th day, 21st day, 28th day, 36th day, 43rd day, 50th day, 57th day and 64th day. The composting period has been set at three months.

Monitoring of the composting process

Turning times correspond exactly to a fixed duration (every two weeks). The windrows were returned four times: two times during the fermentation phase and two times during the ripening phase to promote their homogenization.

In order to optimize oxygen consumption and the production of carbon dioxide in the windrows, windrow turning monitoring is carried out and which includes monitoring of physicochemical

Figure 4. Thermometer used on windrows.

parameters such as temperature, hydrogen (pH), organic matter (OM), humidity and some metals, followed by the evolution of oxygen (O_2) and carbon dioxide (CO_2). Monitoring of pH, organic matter (OM) and humidity is carried out weekly. The temperature was measured daily using a thermometer (Figure 4).

The pH was measured on an aqueous suspension using a Metrohm brand pH meter according to the AFNOR NF ISO 10-390 standard method (Belyaeva and Haynes, 2009).

The humidity (% H) was determined according to the standard Afnor NF U 44-171 method of October 1982 by formula 1:

$$\%H = \frac{M_0 - M_1}{M_0} \times 100 \quad (1)$$

M_O: mass of the raw sample (g); M_1: mass of the sample after passage in the oven (g); % H: percentage of humidity contained in the sample.

The total organic matter content (OM in % of DM) was determined by the loss on ignition according to standard NF U 44-160 of November 1985 by formula 2:

$$\%MOT = \frac{M_1 - M_2}{M_1} \times 100 \quad (2)$$

M_1: mass of the sample after passage in the oven (g); M_2: mass of the sample after calcination (g);-% MOT: percentage of organic matter contained in the sample

The levels of metallic trace elements were determined by flame atomic absorption spectrophotometry (Krou et al., 2019).

The O_2 and CO_2 were monitored using an adaptation of the Sprint V_2 device which measures the combustion gases. The "Sprint V_2 gas analyzer" is a device that not only measures oxygen levels but also carbon dioxide (CO_2) and carbon monoxide (CO) levels. The Sprint V_2 is designed to detect gas leakage in industrial installations. In this work we have made an adaptation of this device. The probe is fitted with a galvanized tube. This tube is made of metal and gives resistance to heat and decomposing windrow materials, which prevent damage to the probe. The tube closed at one end is pierced with small holes around the circumference to allow gas to enter, which is trapped by a rubber stopper closing the other end through which the probe is immersed when a sufficient quantity of gas is stored. The galvanized tube of the device is immersed in the swath and the oxygen level is read when the value stabilizes. Three different measurements are made on the same pile and the average value is retained. Figure 5 shows the measurement diagram.

The oxygen level was assessed using the devices shown in Figure 6.

RESULTS

Monitoring of the composting process

Monitoring of pH, organic matter (OM) and humidity is carried out weekly (Table 1). Figure 7 shows the rate of reduction of organic matter as a function of time. Figures 8 and 9 show the evolution of oxygen and carbon dioxide respectively for windrows A and B. Figures 10 and 11 show the evolution of oxygen and carbon dioxide respectively for windrows C and D. Figure 12 shows the correlation between temperature and oxygen consumption (windrow E).

Metallic trace element content

Table 2 shows the levels of metallic trace elements in the composts.

DISCUSSION

Monitoring of the composting process

Monitoring the pH is an indicator of the degree of biological and biochemical decomposition (Damien, 2004). Indeed, the results show that the pH increases slightly over time and is between 7.4 and 8.5 for windrows. These values are in the range of values obtained for a complete and successful process of composting biodegradable waste which is 8-9 (Koledzi et al.,2019; Sundberg et al., 2004). The increase in pH values is believed to be due to the release of ammonium ions during the process ((Tchanaté et al., 2017); Tang et al., 2004). As for the water or moisture content (H%), the optimum is between 40 and 60% for all windrows; this interval being favorable to aerobic decomposition

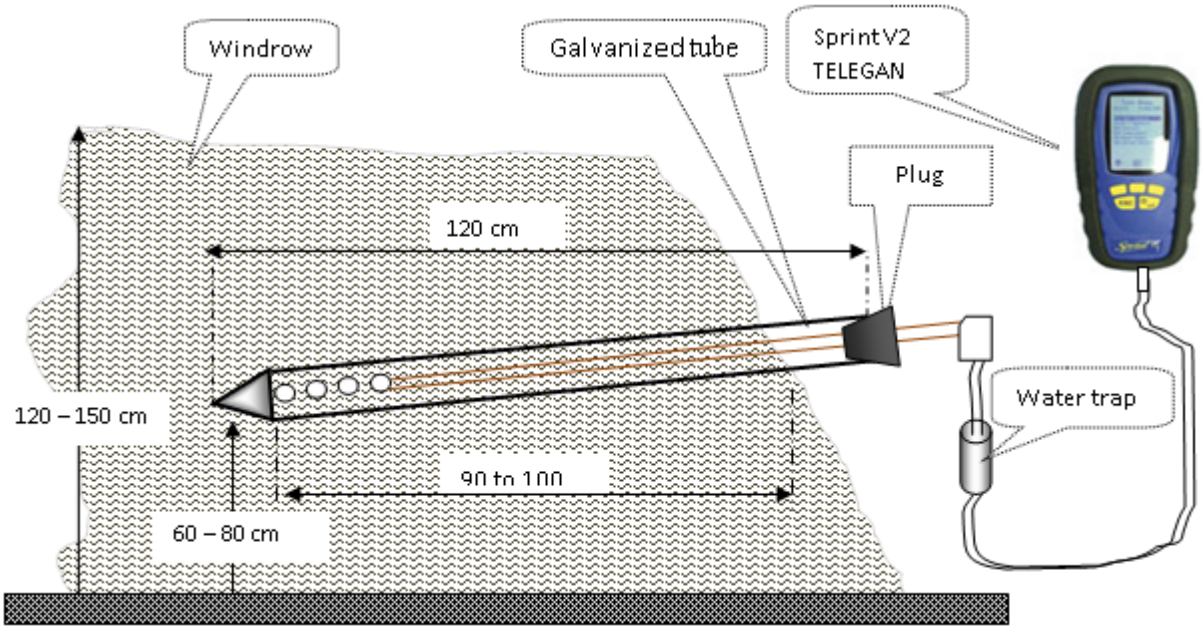

Figure 5. Measurement of O_2 and CO_2 in a windrow.

Figure 6. Device for measuring the oxygen level.

Table 1. Evolution of the parameters influencing the decomposition of organic matter.

	A					B					C					D				
Weeks	0	2	4	6	8	0	2	4	6	8	0	2	4	6	8	0	2	4	6	8
pH	7.5	7.5	7.8	8.5	8.5	7.3	7.6	8	8	8.1	7.5	7.6	7.8	7.9	8.2	7.4	7.8	7.8	7.9	8.1
%MO	62	50	45	35	35	52	43	40	35	32	65	60	58	56	49	67	63	60	55	51
%H	45	50	37	49	51	55	52	44	47	39	43	60	55	40	43	62	51	54	44	40
O_2		13	14	14	8	-	11	14	4	8	-	6	12	14	14	-	6	12	14	16
CO_2	-	3	6.7	3	7	-	1.4	2	14	4	-	9	3	2.1	3.8	-	10	3	2.1	3.8

pH: potential of Hydrogen; % OM: rate of organic matter;% H: rate of humidity; O_2: oxygen; CO_2: carbon dioxide.

(Krou et al., 2019).

Regarding the organic matter content (%OM), it decreases and after eight weeks of activity it is around 35% for windrow A, 32 % for windrow B, 49 % for windrow C and 51% for windrow D. The organic matter contents obtained for the four windrows comply with standards NFU44-051 and NFU 44-095 and indicate that the compost obtained is mature and stabilized for use as a

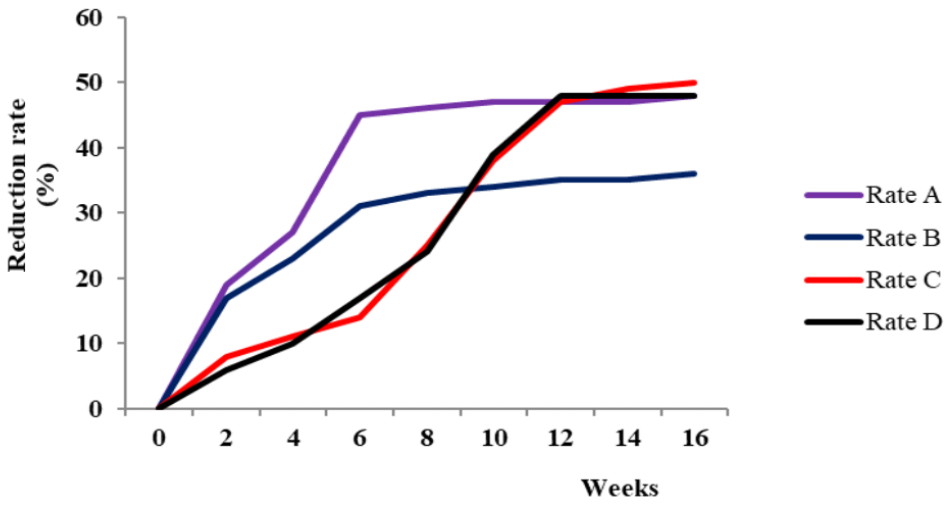

Figure 7. Organic matter reduction rate as a function of time.

Table 2. Metallic trace element content in composts.

Elements (mg/kg MS)	Compost windrow A	Compost windrow E	NFU 44-051
Pb	53	35	180
Ni	10	14	60
Cd	1	Nd	3
Cu	8	10	300
Zn	50	30	600

soil amendment (Rafolisy, 2015).

Figure 7 shows the rate of reduction of organic matter as a function of time.

In terms of the decrease in the organic matter content during the composting process, the results show that the loss of OM after eight weeks (Figure 7) is 46 % for swath A, 33 % for B, 24 % for C and 25 % for swath D. After eleven weeks, only a slight reduction rate (Figure 2) is observed for A and B, that is, 48 and 36%, respectively, whereas 49% is noted for C and 48 % for D on the same date. This result shows that the fermentation is therefore completed after seven weeks for A and B while it continues for C and D up to eleven weeks as shown by the abatement rates (Figure 7). This shows that composts A and B have entered the maturation phase after seven weeks while it is observed for composts C and D after 11 weeks where the mineralization of the organic matter normally becomes slower than the fermentation phase. The decomposition of organic matter is therefore slow in composts C and D compared to composts A and B. The content at the end of maturation is on average 33 % for composts A and B and C and 35 % for D relative to the dry matter. These decreases in organic matter are characteristic of the degradation of organic matter and are strongly related to oxygen consumption and carbon dioxide production. They are also linked to the mineralization of organic matter by microorganisms (Aziablé et al., 2017) with respect to the variation in humidity. In the present study, the decrease in organic matter and therefore degradation and mineralization of organic matter is influenced by the turning method. The frequency of turning in the C and D swaths favoring a high oxygen content and a low production of carbon dioxide slows the rate of degradation and therefore the time of the composting process. Temperature monitoring confirms this development. After each inversion, it is between 60 ° C and 70 ° C for the first seven weeks and then stabilizes between 35 ° C and 45 ° C even without inversion for the swaths A and B. For the swaths C and D, the values between 60 ° C and 70 ° C go up to 11 weeks.

Figures 8 and 9 show the evolution of oxygen and carbon dioxide respectively for windrows A and B.

Regarding the monitoring of O_2 consumption and CO_2 production, Figures 8 and 9, show that the oxygen level repeatedly drops each week compared to the carbon dioxide level until the 53rd day of the week. composting for swath A (Figure 8) and up to day 62 for swath B (Figure 9). The activity of aerobic microorganisms is very intense. Overconsumption of oxygen is frequently

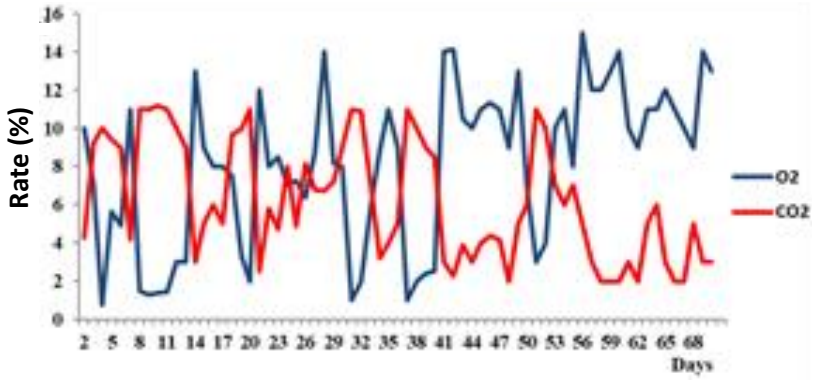

Figure 8. Evolution of O_2 and CO_2 in windrow A.

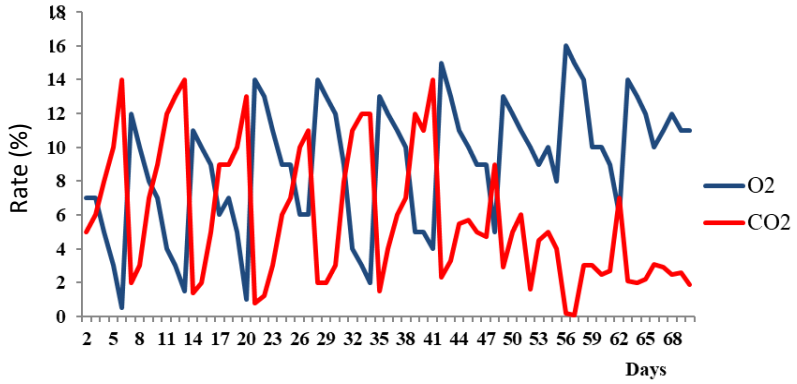

Figure 9. Evolution of O_2 and CO_2 in windrow B.

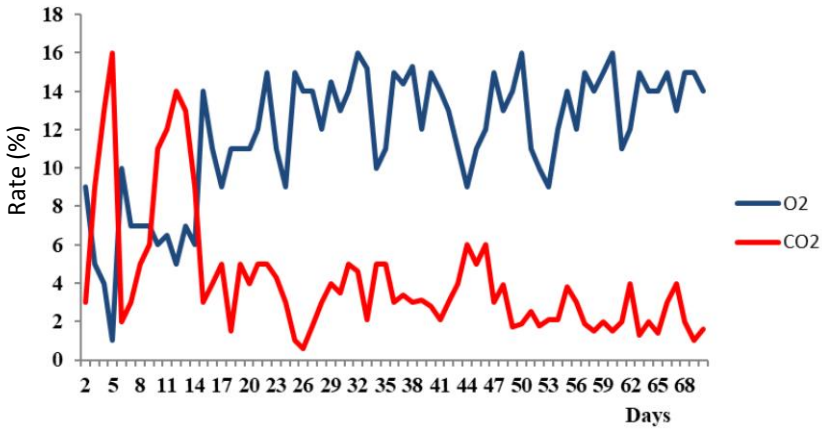

Figure 10. Evolution of O_2 and CO_2 in the Windrow C.

observed in windrows A and B and exceeds the limit for aerobic decomposition of 5% (Puyuelo et al., 2010). Figures 5 and 6 show that the oxygen level for windrows C and D rises above 5 % from the 10th day (Figures 10 and 11) and above 8 % from the 15th day which is the lower rate under carbon finance. Although the activity of aerobic microorganisms is very intense, it is noted that the decomposition proceeds very slowly because the activity started inside the swath is often interrupted by turning especially during the first two weeks. This result

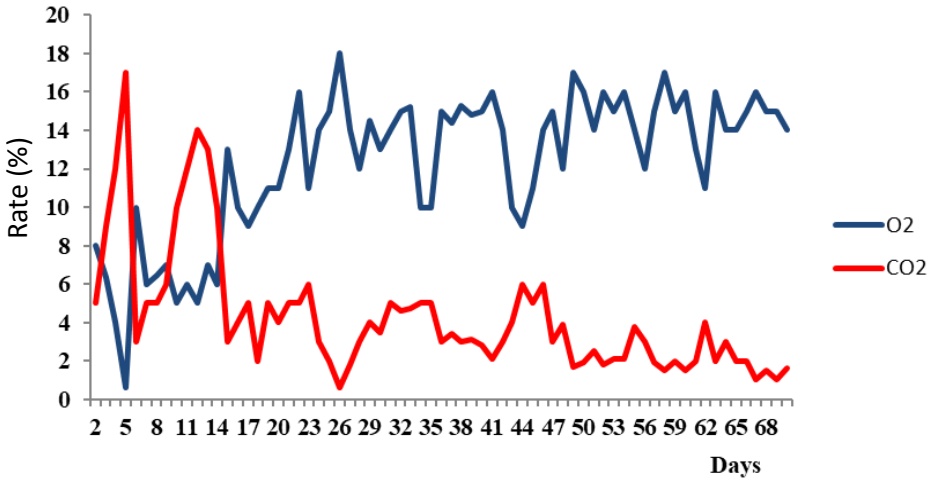

Figure 11. Evolution of O_2 and CO_2 in the Windrow D.

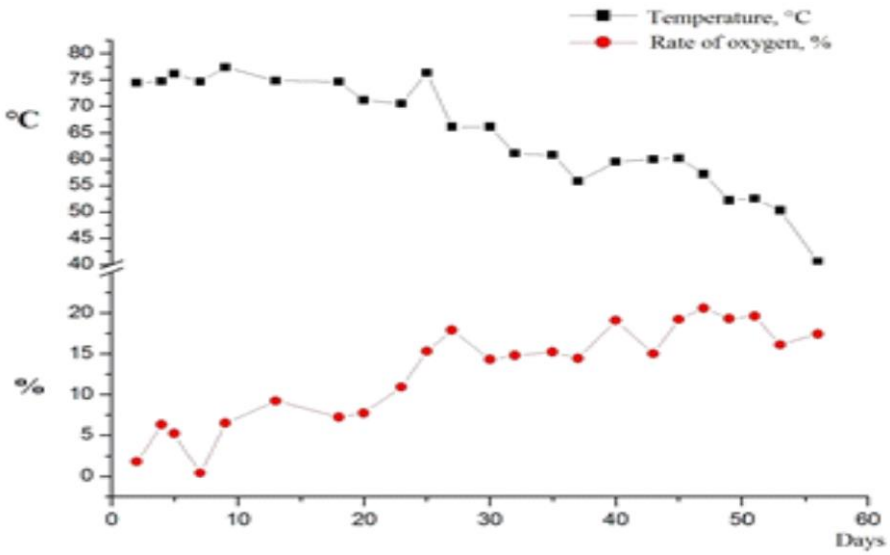

Figure 12. Relationship between T °C and O_2 in the Windrow D.

shows that there is a correlation between temperature, oxygen level and rollovers. In fact, in windrows A and B, there is a decrease in temperature over the weeks with accentuated variations just after the turnings (Figure 12). These also act on the oxygen level measured in the windrows which, unlike the temperature, increases over time, tending towards the content of the ambient air and showing the maturity of the compost. In addition, depending on the method of turning, the variations differ; they are more accentuated when the turns are more frequent (windrow E) than if they are spaced (windrow A). The decrease in biological activities in the heaps is believed to be the cause of the decrease in temperature and the increase in oxygen content. This is more accentuated when the turns are close together.

Metallic trace element content

The analysis of TME (Pb, Cd and Ni) carried out on the composts gives very low values compared to the threshold values of standard NFU 44-051 (Table 2): less than 60 mg/kg DM for Pb, Cd is not detected and less than 15 mg/kg DM for Ni. These low levels are probably linked to the sorting method which considerably reduces the quantity of fines before windrowing. Since composts are free from TME, they can therefore be used without risk of polluting the soil or the food chain through the

products that can be obtained after their use.

Conclusion

The objective of this study is to optimize oxygen consumption and the reduction of organic matter in waste during the fermentation phase. To do this, windrow turning is monitored, which includes monitoring of the consumption of oxygen (O_2), the production of carbon dioxide (CO_2), the temperature, the organic matter (OM), humidity, pH and some metals.

Temperature monitoring shows a gradual decrease until stabilization at room temperature, indicating the maturity of the compost. With a slight increase in all swaths, the pH remained alkaline.

The humidity in the windrows is acceptable, thus promoting good aerobic degradation of the composted waste.

The organic matter in these windrows has decreased to values which agree with the reference despite the fact that the turning mode had a strong effect on the degradation of the waste.

The present study highlights the importance and influence of the oxygen content and the production of carbon dioxide on the mineralization of organic matter, especially in the fermentation phase. The oxygen level obtained inside the windrows is above the limit thanks to the new turning method implemented on the platform in Lomé which is less tedious and which guarantees an oxygen level above 8% throughout the composting process. The decrease in biological activities in the heaps could be the cause of the decrease in temperature and the increase in oxygen content. The oxygen content is necessary for the degradation and mineralization of organic matter but the rate of evolution of organic matter is low when the turning is carried out according to this new scheme, therefore when the oxygen supply is high. We may therefore think that there is an upper limit at which the oxygen level must be maintained to reconcile aerobic decomposition and rapid mineralization. It will be interesting in future investigations to seek the maximum oxygen level that can allow aerobic decomposition and rapid mineralization.

The content of metallic trace elements has also been researched and gives composts that are non-toxic and can be used in cultivable areas.

CONFLICT OF INTERESTS

The authors have not declared any conflict of interests.

ACKNOWLEDGEMENT

This work received financial support from the French Funds for the World Environment (FFEM)/UICN, of the Suez Funds, of the French Agency of Development (AFD) and of La Region Iles de France. The author appreciate the Head of the Laboratory of Waste Management,Treatment and Recovery (GTVD) in which this work was carried out.

REFERENCES

Aziablé E, Tchegueni S, Bodjona MB, Degbe AK, Zamama M, Hafidi M, EL Meray M, Kili KA (2017). Valorization of agro-industrial waste by bio-process aerobic “composting”. Journal of Materials and Environmental Sciences 8(4):1277-1283.

Belyaeva ON, Haynes R (2009). Chemical, microbial and physical properties of manufactured soils produced by co-composting municipal green waste with coal fly ash. BioresourceTechnology 100(21):5203-5209.

Bokobana A, Toundou O, Kolani L, Amouzouvi KAA, Koledzi E, Tozo K, Tchangbedji G (2017). Treatment of household waste by co-composting with the legume Cassia occidentalis L. and some local adjuvants to improve the agronomic quality of composts. Waste Science and Technology-N ° 73-May 2017. https://doi.org/10.4267/dechets-sciences-techniques.3551.

Damien (2004). « Waste management guide, 3rd edition » (Vol. 431). Paris, France. ISBN: 978-2-10-074719-1.www.dunod.com

Koledzi KE (2011). Valorization of solid urban waste in the districts of Lomé (Togo): methodological approach for a sustainable production of compost. Unique PhD thesis, University of Limoges N ° 04-2011. P 118. https://scirp.org/reference/referencespapers.aspx?referenceid=2928623

Koledzi KE, Aziablé E, Megnassan S (2019). Comparative study of the evolution of mass balance on the ENPRO composting platform in Togo. Journal of Chemical, Biological and Physical Sciences Section D 1(9):127-137.

Krou NM, Baba G, Martin-Pascual J, Zamorano TM (2019). Stabilisation co-composting dry drain sludge with fermentescible fractions of household garbage from the city of Sokodé (Togo). International Journal of Biological and Chemical Sciences 13(7):3234-3246.

Mustin M (1987). Compost: management of organic matter. ED. François Dubusc, Paris 954 p.

Puyuelo B, Gea T, Sanchez A (2010). A new control strategy for the composting process based on the oxygen uptake rate. Chemical Engineering Journal 165(1):161-169.

Sánchez A, Artola A, Font X, Gea T, Barrena R, Gabriel D, Ángel M, Sánchez-Monedero, Roig A, Cayuela ML, Mondini C (2015). Greenhouse gas emissions from organic waste composting. Environmental Chemistry Letters 13(3):223-238.

Sundberg C, Smars S, Jonsson H (2004). Low pH as an inhibiting factor from mesophilic to thermophilic phase in composting. Bioresource Technology (95):145-450.

Tang JC, Kanamori T, Inoue Y, Yasuta T, Yoshida S, Katayama A (2004). Changes in the microbial community structure during thermophilic composting of manure as detected by the quinone profile method. Process Biochemistry (39):1999-2006.

Tchegueni S, Kili AK, Bodjona M, Koriko M, Hafidi M, Baba G, Tchangbedji G (2012). Effects of composts based on citrus waste and shea cake on the availability of soil phosphorus: a study under conditions controlled. International Journal of Biological and Chemical Sciences 6(3):1381-1389.

Tchanaté KN, Segbeaya KN, Koledzi KE, Baba G (2017). Evaluation of the physicochemical and agronomic quality of the composts of urban waste of the towns of lome and Kara in Togo. European Journal of Scientific Research 147(4):469-474.

Toundou (2018). Evaluation of the chemical and agronomic characteristics of five waste composts and study of their effects on the chemical properties of the soil, the physiology and the yield of corn (*Zea mays* L. Var. Ikenne) and tomato (*Lycopersicum esculentum* L. Var. Tropimech) under two water regimes in Togo.

Unique doctoral thesis from the University of Lomé in joint supervision with the University of Limoges. PhD thesis: Applied Plant Biology; Specialty: Plant Physiology P 214.

Turan NG, Ergun NO (2008). The effets of aération modifications on municipal solid waste composting. Fresenius Environmental Bulletin 17(7A):778-785.

Rafolisy T, Thuriès L, Técher P, Moussard G, Paillat JM (2015). « Co-composting of beer sludge and livestock manure in Réunion: hygienization, loss of nutrients and homogeneity of the compost produced. Biotechnology, Agronomy, Society and Environment 19(4):329-337.

Related Journals: